


An integrated framework of open-source tools for designing and evaluating green hydrogen production opportunities

Muhammad Haider Ali Khan¹, Phoebe Heywood², Aaron Kuswara², Rahman Daiyan^{1✉}, Iain MacGill^{2✉} & Rose Amal¹ 

Extensive scaling of green hydrogen to meet net-zero targets would need the integration of suitable resources, high renewable energy potential and achievement of supporting techno-economic parameters to establish viable hydrogen projects. Herein, we propose a comprehensive four-tier framework based on specially designed open-source tools that build upon existing knowledge by providing (i) zoning filters to identify potential green hydrogen hubs, (ii) Multi-Criteria Analysis to compare and rank the selected sites, (iii) a production cost tool that allows analysis of 24 different electrolyzer - powerplant design scenarios and (iv) a python based algorithm that establishes the capacity mixes of electrolyzer, powerplant and battery energy storage system required to achieve cost or operational capacity factor targets. The framework is then applied to Australia, where 41 potential sites are used as a case study for comparing their green hydrogen generation potential and costs, benchmarked against international targets of \$2 kg⁻¹.

¹ARC Training Centre for The Global Hydrogen Economy & School of Chemical Engineering, The University of New South Wales, Sydney, NSW 2052, Australia. ²Collaboration on Energy and Environmental Markets and School of Electrical Engineering and Telecommunications, The University of New South Wales, Sydney, NSW 2052, Australia. ✉email: r.daiyan@unsw.edu.au; i.macgill@unsw.edu.au

Green hydrogen (H_2) generated via renewables-driven electrolysis is increasingly emerging as a key driver for deep-rooted decarbonization, especially in energy-intensive and hard-to-abate sectors where direct electrification is challenging e.g., the chemical industry (e.g. methanol, ammonia production etc.) and generation of synthetic fuels for use in aviation or shipping^{1–3}. However, for green hydrogen to become a scalable and viable energy carrier or chemical feedstock (for both export and domestic utilization) there is the need to achieve economic parity with the more established fossil-fuel-based hydrogen production pathways (i.e. Steam Methane Reforming-SMR and Coal Gasification), and the energy sector more generally. Key opportunities for cost reductions include decreasing renewable electricity pricing and electrolyzer costs, optimizing financing costs (linked to technology and market risks), finding the right market fit (i.e. end use and location for best resources to assist hydrogen generation) as well as optimizing overall system configurations including capacity utilization^{4–6}. Currently renewable energy generation costs, particularly of wind and solar, continue to fall with technical progress and achievement of economies of scale, leading them to already becoming the lowest cost sources of new electricity provision in many locations^{7,8}. Similarly, electrolyzers despite still being in their earlier stages of commercial deployment, are also undergoing a rapid cost reduction with technology development and manufacturing scale-up, with further reductions expected as the green hydrogen sector grows^{9,10}. Combined both these factors are expected to drastically reduce the cost of generating green H_2 , and some predictions have it reaching the same costs as fossil fuel-sourced H_2 by as early as 2030, especially in regions with abundant high-quality renewables and favourable financing environments^{10,11}. In the meantime, generally, while the cost of technology remain high, any viable investment into renewables-driven green hydrogen production will require supportive policies, premium pricing and, also, the most efficient utilization of low-cost renewables and what are still capital-intensive electrolyzers.

One key challenge for an efficient and direct integration of electrolyzer and low-cost renewable power generation through solar PV and wind, is their highly variable and somewhat unpredictable nature which restricts the electrolyzer operation to follow the local wind and/or solar power generation patterns¹². Enforcing an economic penalty associated with leaving these capital-intensive electrolyzers sitting idle or operating at limited power for large portions of the year when renewable energy resources are scarce, resulting in lower capacity factors, limited capital efficiency and higher Levelized Costs of Hydrogen (LC_{H_2}). In addition to the economic advantage, high-capacity factor operation of the electrolyzers is also important for the utilization of H_2 , especially for conversion into ammonia or methanol etc. as these conversion processes are currently designed for fairly steady state operation and thus require a stable supply of H_2 ^{13,14}. Integrating them with highly variable electrolyzer operation would then require the inclusion of high volumes of intermediate H_2 storage, which is generally costly to build and suffers from safety concerns¹⁵. Therefore, the optimization of electrolyzer capacity factors is a key research and industry challenge for improving green hydrogen economics.

Yet, the advantages of high electrolyzer capacity factor operation must, however, be weighed against the costs of the renewable generation it draws up. This aspect becomes more prominent and critical when considering actual project design as several configurations of electrolyzer and powerplants can be realized each with its own advantages and disadvantages. Several studies have explored the use of local and wind profiles to simulate H_2 generation and optimise the capacity factor of the powerplants^{16,17}, which suggest oversizing the solar/wind powerplants to the capacity of the electrolyzer, inclusion of hybrid designs with combined solar and wind powerplants^{18–20},

intermediate storage through Battery Energy Storage Systems (BESS)²¹ or Pumped Hydro Energy Storage (PHES) to achieve higher capacity factor operations. However, these studies reveal a trade-off between the high upfront capital investment required to develop these configurations and the ultimate benefit of the increased capacity factor. Therefore, currently, developing stand-alone projects is the most prominent industrial strategy as it allows the electrolyzer to be integrated to dedicated solar/wind farms in regions of excellent wind and/or solar resources (specially sized for optimized capacity factors), water availability, low-cost natural hydrogen storage (e.g. salt caverns) and high land availability, as well as other relevant infrastructure including ports for export, natural gas pipelines for hydrogen injection or local hydrogen demand, e.g., for ammonia generation or decarbonization of local industries (e.g. clean electricity generation, for mobility (fuel cell vehicles) and green steel making etc.).

Alternatively, complex project designs involve isolated systems with fully dispatchable generation, where low cost but variable renewable power is supplemented with multiple energy sources or generally high cost yet more reliable power sources (particularly from fossil fuels) to achieve higher capacity factors while trading-off electricity costs to avoid high LC_{H_2} ¹⁶. One such strategy involves contracting electrolyzers with one or more renewable projects through Power Purchase Agreements (PPAs), while such contracts vary markedly by jurisdiction and involve complexities around regional pricing differences, they typically provide a measure of electricity price assurance if electrolyzer operation is matched to the aggregated contracted renewable generation. Therefore, electrolyzers can operate through time-matched consumption with available renewable generation contacted through PPAs and thus represent the ‘best case’ assured green electricity supply at low cost. Our previous work has studied this in detail and shows that an efficiently volumed electricity supply through a renewable PPA can lead to very high-capacity factors at lower LC_{H_2} s¹⁶. Moreover, there is no obligation that the contracted PPA capacity matches the electrolyzer capacity, thus if their supply exceeds the electrolyzer rating at times and the excess electricity can be sold on to the grid for additional income²², or potentially stored e.g., via onsite battery storage to further enhance their capacity factors²¹, or to operate downstream systems (compressors, etc.). Alternatively, such PPAs can be negotiated to use excess otherwise curtailed renewable generation through the grid, effectively offering zero cost energy supply, but this could still lead to low capacity factors as curtailed energy volumes are also variable and time restricted^{12,23}. Therefore a fossil fuel-complemented grid connection could be preferred as it would permit electrolyzer operation to leverage a stable energy supply above the varying level of contracted renewables. While this would increase electrolyzer operational capacity factor, additional costs of grid connection along with potential issues of network constraints and risk of variable spot pricing as well as environmental concerns of relying on fossil-fuel generation (associated emissions with green H_2) would have to be considered.

Collectively, these prior studies provide valuable strategies to improve capital utilization and reduce the costs of renewable-driven electrolysis. However, the applicability of these strategies is highly context specific due to varying local renewable energy potential, available resources (especially water), and infrastructure (end users and transmission/transport networks). Moreover, in practice as suggested above, there is a wide set of options available to project proponents for integrating renewable supply with an electrolyzer through possible mixes of renewable generation (i.e., battery storage (BESS) inclusion, grid connection or a hybrid combination of solar and wind) and oversizing these with respect to electrolyzer capacity. Thus, there is a clear need for an overarching framework, which provides a systematic approach to evaluate underlying factors that affect the suitability of a given location for developing green electrolyzer projects, and the range

of configuration options available. To the best of our knowledge a number of tools including the H2A analysis tools developed by the US Department of Energy^{24,25}, the AusH2/Hydrogen Economic Fairways Tool (HEFT) developed by the Australian Government²⁶, the Global H₂ Cost Tool developed by the University of Cologne²⁷ and others²⁸, are available that intend to assist developers in assessing potential H₂ generation projects. Each with its own functions and competencies, but a critical overview reveals that these have widely differing scopes, open-source capabilities, and underlying assumptions (refer to Supplementary Note 1 and Supplementary Data 1), which leads to inconsistencies for their application.

To address these limitations, we propose a framework that builds upon the existing strategies and tools, implemented via integrated open-source tools that has been designed for a comprehensive spatial and temporal technoeconomic analysis of renewable-powered electrolysis opportunities. The framework has the following competencies: (i) zoning filters that provide guidance for selecting potential project sites, (ii) a Multi Criteria Analysis (MCA) for a comparative and competitive analysis of each sites to shortlist the sites based on their suitability to host H₂ generation hub, (iii) an open source cost tool that assesses project economic viability by (iv) modelling local H₂ generation potential (over various time resolutions) based on the solar and wind traces in any given location over a year or more, (v) allowing the user to explore a wide variety of renewables—electrolyzer configurations (standalone or grid connected, either solar or wind powered or hybrid combinations with different levels of oversizing and with optional inclusion of BESS storage), while (vi) providing complete control to the user to define/explore various costs (including capital cost of equipment and installation/land, influence of economies of scale, etc. and operating parameters including electrolyzer load ranges, efficiency variations vs load, degradation, etc.), as well as (vii) a python code based algorithm that evaluates benchmark value capacity mixes and cost parameters needed to achieve low LC_{H₂} or high capacity factor operation. In this manner, our framework is designed to provide a user an integrated ‘first pass’ for a convenient and comprehensive assessment of different renewable-powered H₂ generation opportunities.

Herein, we apply the framework to Australia, which is one of the world’s fastest-growing renewable energy markets and a key early player in green H₂ progress. A potential that is already globally acknowledged²⁹, and certainly recognized by the Australian Government, which has set a stretch target to bring the cost of generating hydrogen below A\$2 kg⁻¹ (US\$1.4 kg⁻¹)³⁰ and is actively advancing policy, building trade relations and providing, and attracting investment into green H₂ projects³¹. These projects are intended to serve the emerging hydrogen markets in the Asia Pacific region and beyond, especially Germany, Japan and Korea which are exploring opportunities to import Australian-generated H₂^{32–35}. Given this, achieving economic viability for green hydrogen projects in Australia could play a key role in the development of a global H₂ supply chain. Therefore, Australia provides an ideal case study to demonstrate our framework, as we compare 41 potential hydrogen production sites across Australia, evaluate their costs and benchmark them against the Australian target of A\$2 kg⁻¹ (US\$1.4 kg⁻¹).

Results and discussion

Model framework. The open-source framework proposed herein to evaluate green H₂ production costs is represented in Fig. 1. The framework is built around the following key tools:

1. **Zoning filters:** These are specially defined parameters (detailed below) for preliminary shortlisting of potential

locations that might be converted to a renewable-powered electrolysis hub.

2. **Multi criteria analysis (MCA):** An MCA tool (refer to Supplementary Software 1) is developed for a competitive and comparative analysis between various locations based on a range of criteria which includes, renewable energy potential, locational viability (access to sustainable water, infrastructure for transporting H₂ or electricity), proximity to end-use (opportunities for export or serve local demand for H₂) and opportunity for large scale hydrogen storage (salt caverns or depleted oil/gas reservoirs). Based on these factors, the MCA enables the user to qualitatively map out the location of a given location across each category as well as evaluate a quantitative value (a score out of 10) which can then be used as a comparative measure between different sites.
3. **Project design, hydrogen production simulation and cost evaluation tool:** The HySupply cost tool is introduced that has been developed for evaluating different project configurations of solar and/or wind renewables power electrolyzers. This includes a time step simulation of hydrogen generation using local solar/wind power generation traces and different plant designs (including oversizing of power-plant) to assess temporal performance of the electrolyzer (subject to factors including output varying with efficiency changes and degradation) and hence map hydrogen production over different time resolutions—half-hourly, hourly, weekly, monthly, and yearly (depending on trace data provided). Furthermore, the tool establishes the LC_{H₂} of the project (based on user defined technoeconomic parameters) and can also conduct a more detailed business case analysis (net profit, return on investment and payback analysis) which are beyond the scope of this paper.
4. **Best scenario analysis:** A subsequent python-based brute force algorithm (complementary to the HySupply cost tool) is developed that iteratively processes through a set of defined set cost of assumptions, capacity constraints and performance parameter ranges for the electricity supply and electrolyzer to determine the optimum mix for the least leveled cost (LC_{H₂}) or targeted capacity factor operation.

The framework, its subtools, their functionalities and methodologies are detailed in the Methods. In the next sections we apply the framework to Australia as a case study, where the zoning filters are used to determine 41 potential locations for green H₂ hubs, and the MCA is then applied to provide an outlook of each locations’s suitability to host a H₂ project/hub. Afterwards, the excel tool is applied to assess the local solar/wind profiles to determine hydrogen generation potential and assess the costs of a wide range of potential renewable electrolyzer configurations by adopting the current state-of-the-art costs and performance parameters from literature, engagements with technology providers and future predictions. A sensitivity analysis is then conducted to establish key drivers of costs and determine potential for future costs reduction. Finally, the best scenario algorithm is used to determine the least LC_{H₂} that can be achieved under current cost expectations as well as the energy mix required to achieved high-capacity factor operation (>80%). As well as map out the energy mixes required to reach A\$2 kg⁻¹ (US\$1.4 kg⁻¹) target. Note the provided analysis is based on the general understanding of potential hydrogen projects and publicly available technoeconomic data. Nevertheless, we acknowledge that assumptions are subjective to change depending on the preference of the project proponent, therefore all the tools are made available as an open-source resource for user to alter the assumptions/scope of analysis to meet their requirements.

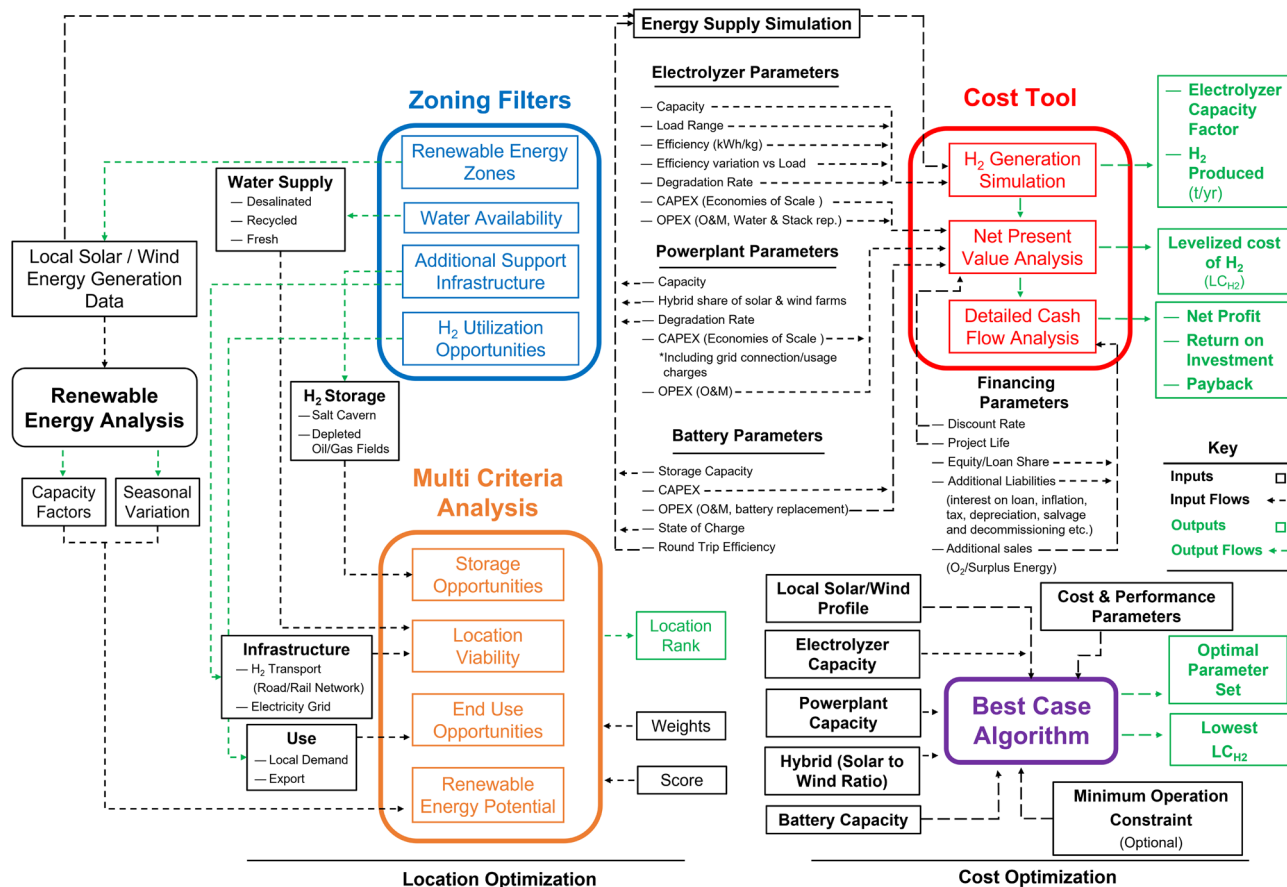


Fig. 1 Schematic representation of the proposed Framework. The framework is based on 4 interlinked tools/tiers; (i) First Tier—the zoning filters serve as guidelines for identifying potential sites for establishing H₂ Hubs, once the sites have been shortlisted each of the selected sites is assigned a rank based on a set of weights and score ranges defined through the (ii) Second Tier—Multi Criteria Analysis (MCA Tool), and then the economics of hydrogen projects envisioned at these sites can be assessed using the (iii) Third Tier—HySupply Cost Tool and these economics can be optimized using the (iv) Fourth Tier—Best case Algorithm that establishes the capacity mixes/power rating of solar or wind or both and BESS capacity required to reach the lowest levelized cost of hydrogen generation (LC_{H₂}) or to achieve a specific LC_{H₂} target or operational capacity factor. Altogether these subtools make up the overall framework which is envisioned as a one stop solution for identifying and evaluating green hydrogen generation opportunities.

Identification of potential sites for electrolysis— use of zoning filters. To develop an electrolyzer facility several critical features would have to be ensured these include (i) a powerplant—source of energy to drive the electrolyzer, (ii) water source—that can provide a sustainable source of water feedstock for the electrolysis, (iii) end use—a demand that can offtake the generated hydrogen and (iv) support infrastructure—that can enable integration of all these resources. As an initial part of our framework, we consider each of the above as a category of zoning filters that act as a guideline to shortlist potential locations, and these are detailed below:

Water availability. A sustainable and scalable water supply is an essential input to electrolyzer systems. Prior work has shown that water costs make only a relatively modest contribution to hydrogen production costs, even if high levels of treatment is required (e.g., desalination)¹⁶. Instead, the availability of a suitable and proximate water source becomes a locational constraint given the environmental considerations (for example, threats to fresh water reservoirs) and the competition with other high priority water uses such as agriculture¹⁶. For our analysis we consider groundwater, desalination and recycled water availability in Australia and cost them on basis of average wholesale pricing (Supplementary Note 2, Supplementary Figs. 1–3 and Supplementary Table 1).

Renewable energy availability. Similarly, access to renewable electricity is another key underlying aspect of green hydrogen generation, therefore potential locations will be constrained by their associated renewable resource potential, available land to install the electrolyzer and any associated plant as well as dedicated solar/wind farms, and infrastructure to support energy projects (transmission lines, BESS etc.). In this regard, regions identified by policy makers as Renewable Energy Zones (REZs) offer key opportunities as they are already designated areas with high renewable energy generation potential, available land that is suitable for project development and suitable energy infrastructure including transmission already in place or planned for development. Several REZs are already identified in Australia, and we consider these for our analysis as shown in Fig. 2. The solar and wind generation potential and their variability across these REZs were used herein as a key metric to compare the regions (refer to Methods, Supplementary Note 3, Supplementary Figs. 4–12 and Supplementary Table 2).

End use. Another factor governing choice of production location is proximity to suitable downstream utilization opportunities. Domestically, we assume H₂ can be used as a feedstock or clean fuel in existing industries, e.g., ammonia production facilities, oil refineries and steel plants, or as a clean fuel for large emitters, e.g., cement facilities, and alumina smelters. Additionally, hydrogen

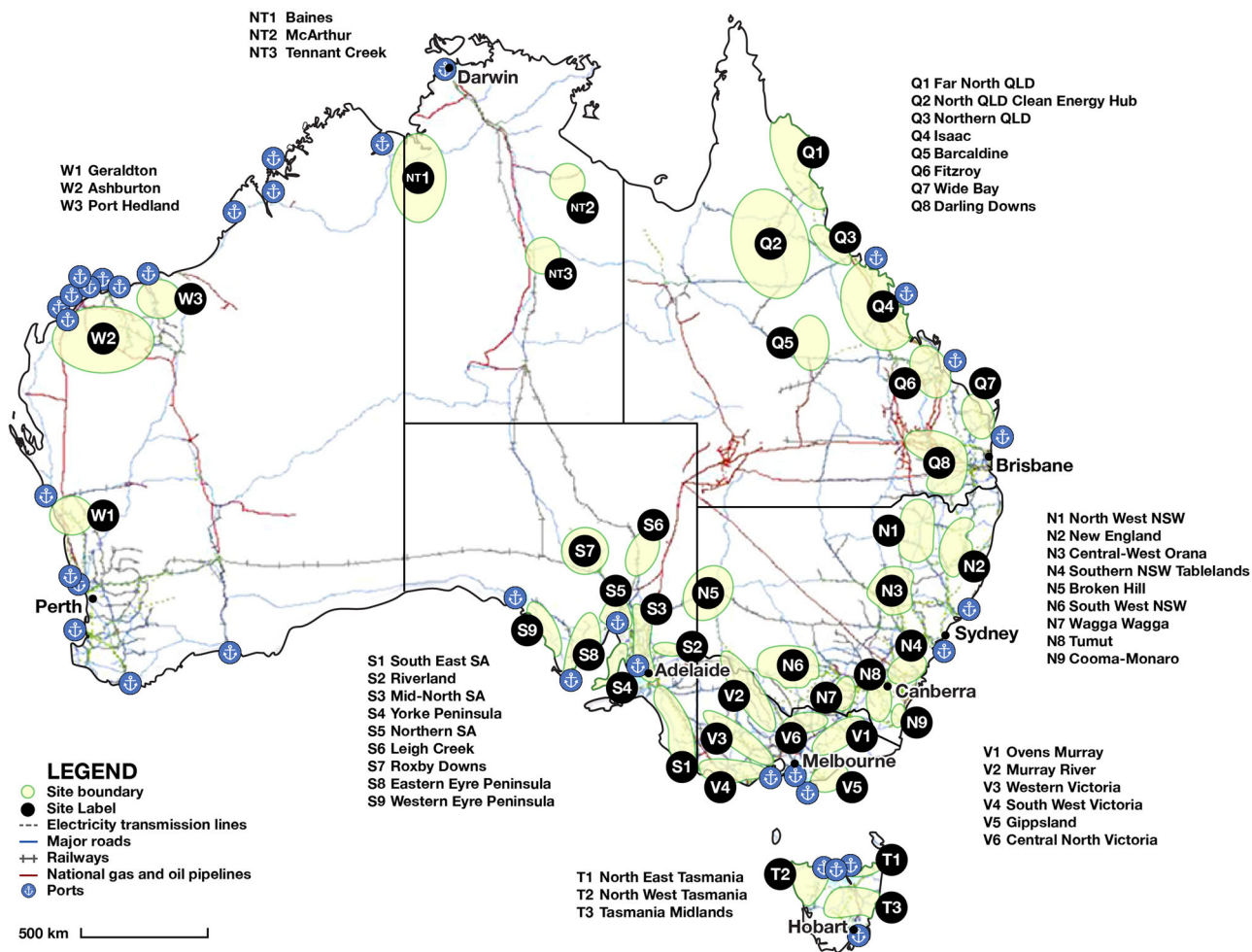


Fig. 2 Map of potential hydrogen generation zones selected for the analysis. The maps show the considered renewable energy zones (potential sites for green electrolysis projects), existing electricity transmission lines, roads, railways, gas and oil pipelines and port infrastructure. The location of the NEM connected REZs were adopted from the AEMO ISP, the rest of the locations for WA and NT were drawn to approximation (region with same solar and wind traces). The data for the infrastructure (road, rail, electricity transmission lines, natural gas/oil pipelines and port locations) and the map of Australia were adopted from data made available by Commonwealth of Australia (Geoscience Australia) under Creative Commons Attribution 4.0 International Licence²⁶.

can also be injected and hence blended into existing natural gas pipelines (already being actively demonstrated in Australia)³⁶. We also assume electrolyzers integrated with solar/wind farms and fuel cells can be used in combined power and heat systems to replace diesel or natural gas fired generators that are actively used in off-grid sites across Australia. More broadly, it seems likely that the bulk of Australia’s hydrogen production may be exported, and sites close to the coast or existing ports with energy export infrastructure (refer to Supplementary Note 4 and Supplementary Table 3) could well end up being used as hydrogen export hubs.

Additional infrastructure. To leverage these various utilization opportunities, additional support infrastructure including intermediate hydrogen storage, transport facilities and electricity transmission networks would be required to integrate the hydrogen generation facility and downstream end use sector. For small scale projects, e.g., hydrogen refuelling stations, viable storage can be realized within the production facility using pressure vessels³⁷, however, with scale, the cost of such storage increases drastically, likely making them unviable³⁸. For large scale storage, salt caverns offer a much more viable solution due to low cost construction, strong containment, low risk of H₂

leakage and fast injection and withdrawal rates³⁹. Similarly, depleted oil and gas reservoirs⁴⁰ or geographical formation suitable for CO₂ storage might also be used for H₂ storage (refer to Supplementary Note 5 and Supplementary Fig. 13)⁴¹. While existing road and railways can be leveraged to transport, the equipment, workforce, and produced hydrogen via tube trailers. As an alternative in the absence of such opportunities, dispatching the electricity from the solar/wind farm from potent locations to the electrolyzer installed at the utilization site might be more viable, for which any existing grid infrastructure could be leveraged albeit at additional cost of connecting to the grid and transmission charges.

We conducted an extensive analysis of all these opportunities across Australia (refer to Supplementary Note 6 and Supplementary Data 2), and through these zoning filters identified 41 particularly prospective hydrogen production locations across Australia as shown in Fig. 2.

Multi criteria analysis tool. The next stage of the framework develops a multi criteria analysis (MCA) tool to conduct a competitive analysis of the selected sites. The MCA considers a range of parameters under different categories presented above, and now elaborated here:

Location viability. This category is based on the data collected from the application of the zoning filters across the considered locations, highlighting the availability of water locally through either groundwater or via water from existing desalination plants or existing recycle/wastewater treatment plant and any existing transport (rail and road) or grid infrastructure (powerlines/proposed) that can be leveraged.

End use opportunities. This subcategory includes access to the coast (potential opportunity to develop a jetty or export terminal for the hydrogen generated), or existing port with established export infrastructure or identified as future hydrogen export port, existing hydrogen demand centre or opportunities for decarbonization (as elaborated earlier), or existing natural gas pipeline for potential H₂ injection or the opportunities to use hydrogen as an electricity generation/storage option (potential to replace existing natural gas/diesel powered generators in off grid locations).

Storage opportunities. In addition, we assess the storage opportunities based on the access to either to a suitable salt cavern or depleted oil/natural gas fields that can be used for H₂ storage.

Renewable energy potential. This category includes comparing the local solar and wind capacity factors as a measure of the site's renewable energy generation potential and their variability as a measure of seasonal variation (intermittency of solar and wind). For the details on how each of these were evaluated are provided in Methods.

Each of these categories was assigned a weighting while each subcategory was assigned a score, which are aggregated to determine the overall rank as shown in Eq. 1:

$$\text{Rank} = \sum_{i=1}^4 W_i \times \left(\sum_{n=1}^z S_n \right) \quad (1)$$

Here W_i represents the weight of the individual MCA category i and S_i represents the score for each subcategory n (with z representing the inclusions within each subcategory). The categories, their assumed weights and scores are elaborated in the "Methods" section. The MCA framework then establishes an overall ranking (aggregated based on weighting across all categories of MCA) for each considered location out of a maximum rank of 10.

We applied our proposed MCA framework to rank and provide an overview of the suitability of the 41 considered locations (Fig. 2) as shown in Fig. 3. A summary of the MCA findings is provided below, while a detailed outlook for all considered REZs is available in Supplementary Note 6 and Supplementary Table 4.

The MCA reveals that some of the more favourable sites for developing hydrogen hubs are available in Queensland (QLD), South Australia (SA), Western Australia (WA), and New South Wales (NSW). Overall, the MCA based ranking results also reveal an interesting trade-off between sites with renewable energy potential, resources (better water, storage opportunities etc) and end use opportunity, highlighting that a high score across all the categories is not guaranteed with some locations having high renewable energy potential but limited complementary resources of water, transmission networks, road/rail connections and potential end users. E.g., as observed most of the high profile solar/wind sites (like Broken Hill, Clean Energy Hub North Qld etc.) are often far off from high value end use opportunities like existing ports or local demand centres or face locational issues especially water availability. However, as suggested earlier these sites can be leveraged for grid connected opportunities where the

electricity generated at the REZs can be transmitted (at the cost of additional grid usage charges elaborated earlier) through the grid to electrolyzers established in suitable locations and close to demand sites. This can also be achieved using the rail and road network, where the hydrogen can be generated at a suitable site and then transported to the utilization site, creating room for additional economic optimization to either develop an electric network or a supply chain. Moreover, the MCA framework also allows us to compare the renewable energy potential and seasonal variability, which highlights that while several sites might have high renewable energy potential but are also susceptible to high seasonal variability which would result in variable H₂ production and affect downstream utilization (e.g. requiring oversizing, grid supplementation or BESS to firm the supply which will be an economic concern as discussed in later sections). Similarly, solar and wind profiles at several locations can play a complementary role e.g., if the solar profile is high volatile and the wind is highly stable these profiles can be combined to make a hybrid powerplant which would have a more stable H₂ supply (as elaborated later).

In addition, as elaborated earlier, it's important to note that the MCA is highly subjective to scope of analysis, as the rankings can vary significantly depending on how the assumptions are set up. Currently, we have set up the MCA with the highest weighting given to renewable energy potential and end use, and with scoring inclined towards factors like higher scores for good renewable potential and low seasonal variation, export as the highest scoring end use and desalination as the most sustainable source of water etc. as these reflect the most likely settings for project development as elaborated in the Methods section. In comparison, the user might prefer the use of hydrogen locally and other locational viability factors e.g., co-location with recycled water facilities etc. as the highest weights, this could significantly change the outlook of the MCA. To enable this the MCA tool (refer to Supplementary Software 1), is made available as an open-source resource to allow the user to update or add their own weights, categories, and score matrix as per requirement. Therefore, such an MCA framework provides a simple yet powerful tool for initial shortlisting of sites that fulfill a specific project scope.

Application of the HySupply Costing Tool. The third stage of the framework is the development and application of the HySupply Cost Tool. The details of the tool are elaborated in the "Methods" section, Supplementary Information, and the sections below. In summary, the tool (refer to Supplementary Fig. 14) is designed to rely on local solar and wind traces to conduct an hourly simulation of powerplant power output (based on combinations of solar/wind farm and BESS) which can be designed in a wide range of scenarios (refer to Supplementary Fig. 15 and Supplementary Table 5), the power output is then co-related with the efficiency of the electrolyzer (refer to Supplementary Fig. 16) to provide the hourly hydrogen generation profile. In this manner, using the tool the capacity factor profiles can then be mapped for all the considered locations to determine and understand the trends of overall hydrogen generation potential at each site as described in the sections below. In addition, the tool can conduct a robust technoeconomic analysis based on user defined capacities, cost, and performance parameters (which include advanced features to design and evaluate 24 different electrolyzer—powerplant configurations listed in Supplementary Table 5, through a comprehensive capital cost—direct and indirect cost model, economies of scale, electrolyzer efficiency variation with load, degradation etc. which are generally not present in other tools as highlighted in Supplementary Data 1). Herein we use the

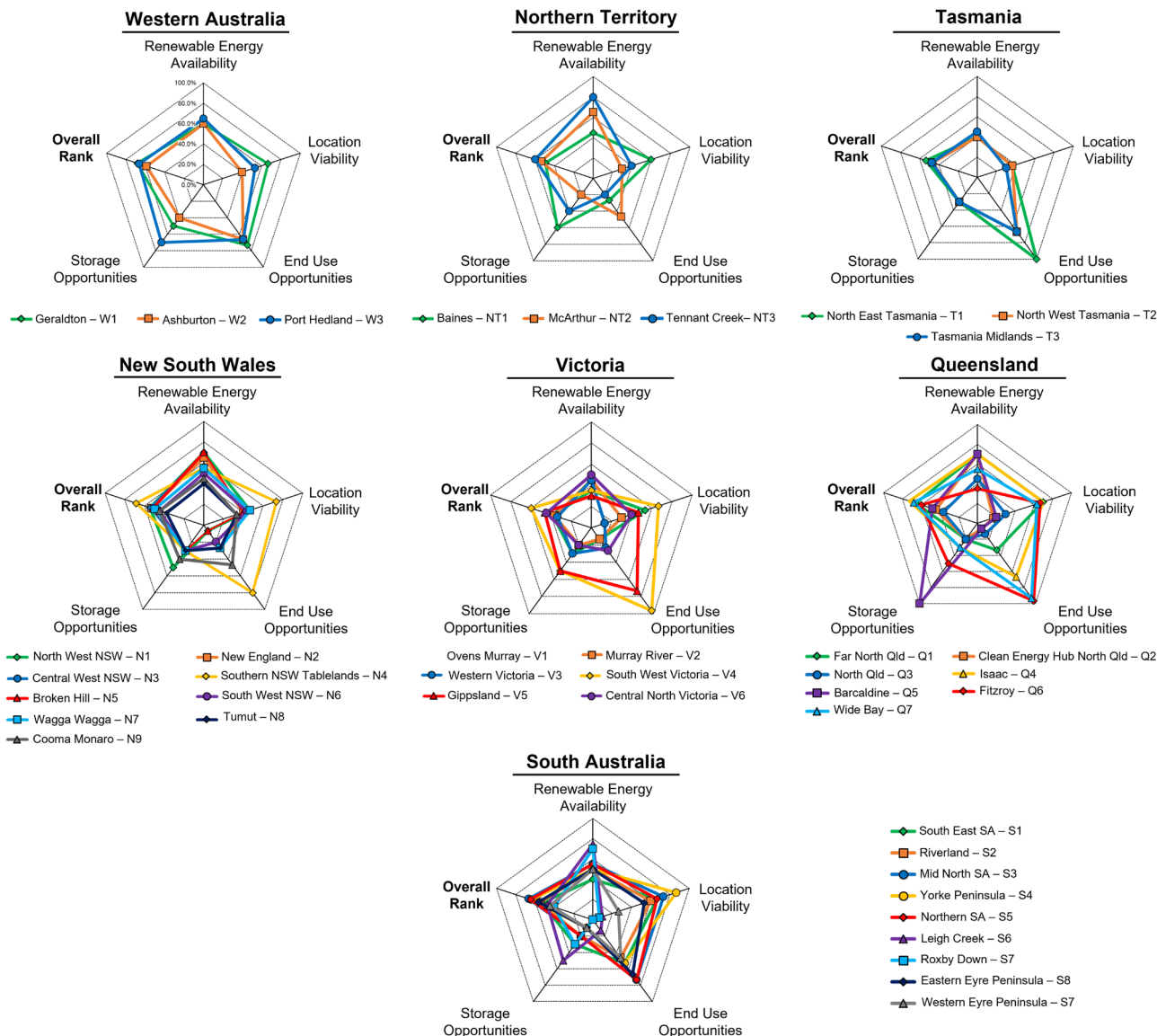


Fig. 3 Results from the MCA Framework. Scores are measured across individual axis of the spider web (solid lines), with each category (overall rank, location viability, etc.) with a score of 0–100% (each dotted line represents an interval of 20%). To read the graph, pick a location (represented with different symbols in the keys for each state) and individual category (renewable energy availability, location viability, end use opportunities and storage opportunities), the score for that category is then measurable how far from the centre the symbol is on the axis. E.g., if we chose Geraldton in WA and measure its score for end use opportunity, we see that the symbol lies close to the 4th dotted line from the centre that represents 80%, so for end use opportunities Geraldton scores 80% out of a max score of 100%. Moreover, the wider the distribution (or the more spread out the solid lines—spider web for any given location), the better it ranks in terms of all categories. The score assigned are assigned to each location based on the matrix in Methods section (Table 3), the complete MCA database and ranking for the individual locations is presented in Supplementary Data 2 and the summary of the MCA results for each state is detailed in Supplementary Table 4.

tool to determine the LC_{H_2} , by adopting literature-based cost and performance parameters as elaborated in “Methods” (refer to Supplementary Tables 6–7).

Geospatial modelling of solar and wind traces. Of all the considered locational aspects, the renewable energy potential is the most critical factor for green hydrogen generation. Our analysis (refer to Supplementary Table 2 and Supplementary Fig. 17) shows that the highest solar profiles are available in Northern Territory (NT), SA, QLD, and WA (and lowest in Victoria—VIC and Tasmania—TAS), with the average solar capacity factors (average of all the considered sites in each state) in order of; (i) WA—33.4%, (ii) NT—32.2%, (iii) QLD—30.5%, (iv) SA—29.2%, (v) NSW—29.1%, (vi) VIC—25.9%, and (vii) TAS—23.8%.

Overall, the highest average solar capacity factor is exhibited in Tennant Creek, NT (capacity factor of 35.5%), while in other states: WA—Geraldton (33.9%), NSW—North West REZ (32.7%), VIC—Murray River REZ (29.8%), SA—Roxby Downs REZ (32.9%), QLD—Barcardine REZ (33.7%) and the TAS—North East Tasmania REZ (25.2%) have the highest capacity factor. Similarly, the average wind capacity factors are in the order; (i) TAS—48.5%, (ii) QLD—44.9%, (iii) NT—38.2%, (iv) SA—38.1%, (v) WA—36.5%, (vi) VIC—36.0% and (vii) NSW—35.4%. The highest wind capacity factor is exhibited by Far North Qld REZ (capacity factor of 58.7%), with similar high-capacity factors are also shown by Tasmania Midlands REZ (55.3%) while the in other states NSW—Tumut REZ (42.2%), VIC—Ovens Murray REZ (41.4%), SA—Leigh Creek REZ

(42.3%), NT—Tennant Creek REZ (48.5%) and WA—Geraldton REZ (43.5%) have the highest capacity factor. Overall, and as expected, wind offers higher capacity factors than solar across all regions. Several REZs in QLD and WA offer interesting case studies as they offer both high solar and wind potential.

However, as elaborated earlier, capacity factor provides limited information on the variability of the solar and wind profiles over time. This is an important consideration for project proponents given how short-term variability will impact on the amount of hydrogen storage required, while seasonal variation will impact on production profiles for delivery to consumers. To the best of our knowledge no other publicly available tool (refer to Supplementary Data 1) analyze variability in capacity factors of local solar and wind traces and their subsequent effect on electrolyzer generation over different time resolutions. Our tool, by comparison, has the functionality to map the locational solar and wind profiles over various resolutions. Here we only focus on monthly distribution curves for simplicity and the fact that they best visualize seasonal variability. To undergo this evaluation, we compare the monthly average capacity factor curves for solar and wind of the best performing location (i.e., highest overall annual capacity factor) vs the worst location (i.e., lowest annual capacity factor) for each site as shown in Fig. 4. Comparing the capacity factor curves highlight that for NT, the maximum daily capacity factors across the months remain between 80 and 100% for both solar and wind, and in the northern region (NT1), the solar traces generally peak in the Australian winter (April–Sept), at the same time in the south (NT3) the solar profiles decline and tend to peak in the tail end of the winter (Sep–Dec). In comparison, the wind profiles also peak between May and Sep in the northern regions (NT1 – NT2) but for the southern regions the profile peak for a larger period April–Sep). In contrast, WA show similar solar profiles near the coast (W1 and W3) with peaking in Australian Summer (Jan and Feb), after which there is a decline and stabilization around the average (March–Jul) before peaking again towards the later part of the year (Aug–Dec). Inland (W2), there is a similar profile, but this location experiences a much higher decline in the mid-year as experienced in the other locations. In NSW, the solar profiles tend to remain high throughout the year peaking in the summer months (especially around Dec/Jan and April) and decrease during the winter months of (June to Aug). While the wind traces across the state show a similar trend with peaking in the winter months (May to August) especially in the southern locations (Tumut and Cooma Monaro REZs). Similar trends can be identified for the rest of the locations.

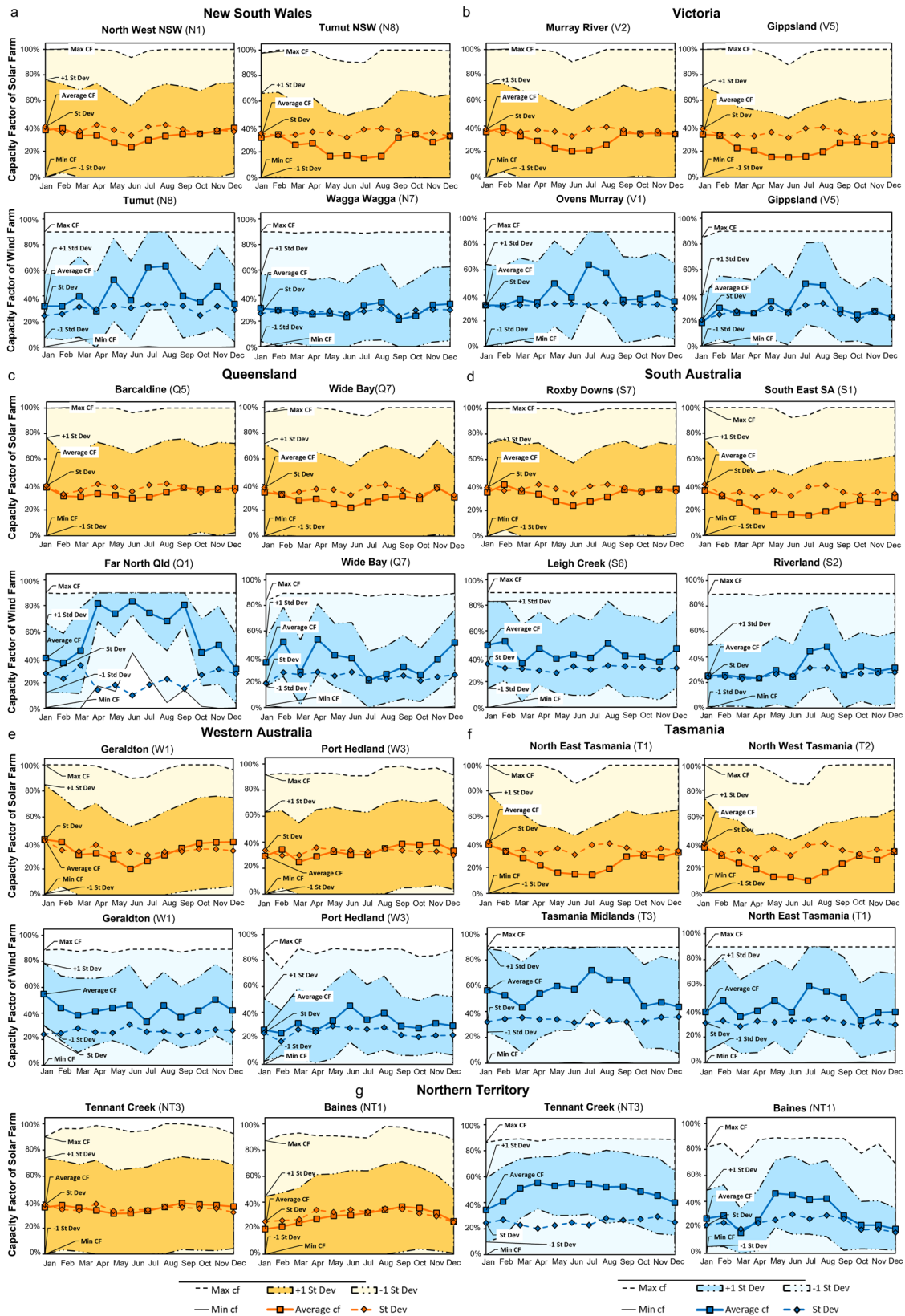
These solar/wind production traces are of interest to project proponents as they assess risks associated with long term downstream hydrogen supply contracts based on long term (monthly) or even shorter volumes (daily). They can be used for a preliminary design for storage capacity, where the annual capacity factor can be used as a standard for yearly hydrogen output (ton/yr) and the trend of daily, weekly, or monthly capacity factors (especially their standard deviations) can be used as potential patterns to define downstream hydrogen supply contracts (e.g., contracts can be scheduled to supply larger volumes of H₂ during months with favorable solar/wind production or to establish storage volumes and durations required to meet baseline supply requirements around the year by storing excess demand during favorable months to offset the lower production in months with variable or low solar/wind production). Moreover, the traces can also reveal sites where solar, and wind play a complementary role both in terms of capacity factors and variability over different time periods to develop a hybrid powersupply that can ensure better capacity factors compared to having either a solar or wind farm operating the electrolyzer. While here we focus on the solar and wind traces

over annual and monthly resolutions for solar and wind farms, the tool also can map similar traces for electrolyzer capacity factor which can be compared to evaluate load variations, efficiency vs load trade-offs as well as impacts of hybrid or oversized powerplants on the electrolyzer.

Base case results. In addition, as a base case, we assess the levelized costs for standalone wind and solar farm powered 10 MW electrolyzers across each site, the results are shown in Table 1. We evaluate that the LC_{H₂} for Solar powered AE systems will range between US\$5.5 kg⁻¹ and US\$8.6 kg⁻¹, while that of PEM system will range between US\$7.1 kg⁻¹ and US\$10.8 kg⁻¹ at present input cost estimates (refer to Supplementary Fig. 17). Similarly, for Wind powered AE and PEM systems the costs range between US\$3.7 kg⁻¹ and US\$7.8 kg⁻¹ and between US\$4.7 and US\$9.2 kg⁻¹ (refer to Supplementary Fig. 17). The lowest average LC_{H₂} (US\$4.7 kg⁻¹ and US\$4.9 kg⁻¹) are recorded in Tasmania and Queensland, for wind driven systems due to the inherent high-capacity factors. Moreover, the AE systems have a lower capacity factor due to a lower operational range compared to PEM, which allows PEM systems to take advantage of lower capacity power outputs from the powerplant and operate for longer times, however AE has a LC_{H₂} advantage due to lower capital cost and lower specific energy consumption (kWh kg⁻¹). Note these values are based on current cost expectations (refer to Methods), and as highlighted in our prior work and that of others, there remains significant room for improvement in costs remain due to capital cost reduction and efficiency improvements¹⁶, as well as taking advantage of scaling project capacity to take advantage of economies of scale and further capacity factor optimization (oversizing, inclusion of BESS and hybrid powerplants).

Scenario and techno-economic parameter sensitivity analysis. To evaluate the potential of LC_{H₂} reduction we use the tool to conduct a sensitivity analysis (scenarios elaborated in Supplementary Table 8) using critical factors (i) capital cost (CAPEX) reduction, (ii) economies of scale, (iii) efficiency improvements and (iv) different electrolyzer–powerplant configurations (Fig. 5).

CAPEX reduction. Prior analysis has shown capital reduction across all three technologies (electrolyzer, solar and wind) are a key driver for LC_{H₂} reduction. The analysis undertaken in this study (Fig. 5a, b) reaffirms this and highlights that cost reductions for the electrolyzer is more important in lowering LC_{H₂} than a reduction in solar and wind powerplant capital costs. Estimates for future electrolyzer costs suggest that these might well be reduced by 50–70%, while those of solar have been forecast to decrease by 50–60%, yet perhaps only around 5–10% reduction in wind power costs (refer to SI section Supplementary Note 8). Our prior analysis has shown that these cost reductions would be a key driver in reducing costs to match the Australian Government's stretch A\$2 kg⁻¹ target (US\$1.4 kg⁻¹)¹⁶. In addition to the upfront capital cost reduction, scaling up projects to higher capacity (>10 MW) will play a further complementary role in reducing the LC_{H₂}, especially if projects of multi MW scales (>500 MW) to take advantage of economies of scale would lead up to 70% reduction in LC_{H₂} under current expectations, and even more if a lower scale index (n) (the unit cost reduction associated with larger projects) can be achieved (Fig. 5c-d). Moreover, while installing electrolyzers at site, additional costs are added to the equipment cost due to installation and land expenses (for both electrolyzer and powerplant plus that of BESS and grid connection if present), while land costs are likely to increase due to the nature of the market, installation costs are likely to decrease as the supply chain for electrolyzers are established. In addition, while



we do not consider this in our modelling, remoteness of the site from major industrial energy hubs could also affect project economics, as prior analysis for renewable projects in Australia show that cost of installation increases if projects are not developed in close proximity to industrial hubs due to lack of local industry capabilities and workforce⁴².

System efficiency improvements. Alternatively, increasing the efficiency of the systems is another a key avenue for LC_{H_2} reduction. Improvement in electrolyzer energy consumptions/efficiencies ($kWh\ kg_{H_2}^{-1}$) are expected with ongoing R&D⁴³, and our sensitivity analysis (refer to Supplementary Fig. 18a) shows this would reduce the LC_{H_2} due to capacity factor improvement

Fig. 4 Variability in the solar and wind traces across the best and worst performing locations amongst the selected REZs in each State. Each set representing the State of **a** New South Wales, **b** Victoria, **c** Queensland, **d** South Australia, **e** Western Australia, **f** Tasmania and **g** Northern Territory consists of four figures that show the site (from amongst the selected sites) with the highest annual capacity factor (on the left), compared to the one with the lowest annual capacity factors (on the right) is shown for solar energy (the top two figures of each set) and for wind energy (the bottom two figures of each set). Note: the statistical data shown in the figure are the minimum (min cf), maximum (max cf) and average capacity factors (Average cf) as well as the standard deviation in capacity factors (Std Dev & ± 1 Std Dev.) are provided across the months of the year at each site, the details of these metrics are provided in the SI. These locations are used as an indicative representation of the general trends in each state (similar figures for the rest of the considered locations are shown in Supplementary Figs. 6–11). Moreover, ~10% loss in output is observed across the wind profiles this is due to system losses elaborated in the “Methods” section.

Table 1 Summary of the base case results.

State	Solar driven system				Wind driven system			
	Capacity factor (%)		LC _{H2} (US\$ kg ⁻¹)		Capacity factor (%)		LC _{H2} (US\$ kg ⁻¹)	
	AE	PEM	AE	PEM	AE	PEM	AE	PEM
NSW	27.64%	28.00%	6.48	8.16	33.80%	35.55%	6.16	7.53
VIC	24.45%	24.90%	7.34	9.21	33.72%	35.33%	6.17	7.63
QLD	29.08%	29.32%	6.14	7.79	43.05%	44.31%	4.97	6.13
SA	27.75%	28.05%	6.48	8.19	35.75%	37.45%	6.13	6.23
WA	28.56%	32.05%	5.61	5.79	34.49%	35.88%	5.69	6.80
NT	27.50%	29.76%	5.87	6.06	36.19%	37.58%	5.32	6.10
TAS	22.31%	22.85%	7.97	9.98	46.49%	47.80%	4.58	5.65

The values represented are the average of the capacity factors and levelized cost of each considered REZs in the mentioned state/territory. The breakdown of the values for each individual REZ is detailed in Supplementary Fig. 17.
The average capacity factors and levelized costs across each state. These standalone systems with individual equally sized solar and wind powerplants, without any BESS.

as more hydrogen is generated for the same energy applied. However, a counter element is the degradation of the electrolyzer and solar/wind farms that leads to lower energy output and subsequent lower hydrogen generation, with our prior analysis¹⁶ shows that these aspects are usually neglected in cost modelling and our sensitivity results show these can add upto 2% increase in LC_{H2} (refer to Supplementary Fig. 18b–c). Similarly, another commonly underexplored aspect is the efficiency variation with load, literature analysis shows that both AE and PEM operate at higher efficiency at lower loads (refer to Supplementary Fig. 16). This could be considerably important as shown by duration curves, as the electrolyzer with dedicated powerplant would operate at lower loads for longer durations as compared to higher loads (refer to Supplementary Figs. 4–11). Our sensitivity analysis reveals that accounting for this can lead upto ~30% reduction in LC_{H2} (Fig. 5e). Specifically, for the PEM electrolyzers, they also can be overloaded (run upto 120–150% of their nominal loads⁴⁴), accounting for this shows that the LC_{H2} can further decrease by 5–10% (refer to Supplementary Fig. 18d).

Configuration designs. The configuration of the electrolyzer and powerplant integration would also influence the LC_{H2} due to different share of each component in the total project costs and the subsequent capacity factors delivered. We have already revealed that an optimum oversize ratio (1.25–1.5) exists for delivering the LC_{H2}¹⁶ and our sensitivity results also support this finding as oversizing by 1.5 leads to cost reduction (Fig. 5e). However, a critical part of the oversizing the powerplant is that excess energy has to be curtailed¹⁶, adding a BESS is a potential solution as suggested earlier. The sensitivity analysis reveals an interesting aspect that while inclusion of batteries and oversizing increases to enhanced capacity factors it also causes increase in LC_{H2} due to additional CAPEX; a premium (higher LC_{H2}) will be incurred for ensuring high-capacity factor operation. However, given the different levels of oversizing and BESS storage (Fig. 5f), an optimum energy mix can exist that allows both high-capacity

factor and acceptable LC_{H2}. Moreover, given there is a capital cost difference between BESS of different power and storage duration, an optimum mix also exists while choosing the batteries rated output—MWh (refer to Supplementary Fig. 18e). Similar trade-off also exists in developing a hybrid powerplant, e.g., in Geraldton (site used as an example for our sensitivity analysis), a hybrid combination can be developed to take advantage of a higher capacity and less volatile wind traces to boost the lower capacity factor and more volatile wind. Our sensitivity result (Fig. 5g) also supports showing that a hybrid powerplant with a larger share of wind has a lower LC_{H2} than that with a larger share of solar, therefore a trade-off also exists between different hybrid ratios due to different capital cost of solar and wind farms (solar farms are less costly than wind farms) and the capacity factors (wind traces mostly higher than solar and less volatile across Australia as compared to solar traces). This is where the best-case scenario algorithm comes as it can run through the range of capacity mixes (solar/wind, oversize ratios, share in hybrid combination and BESS capacity) to find the most optimum mix for LC_{H2} and capacity factor targets as elaborated in the next section.

Alternately, the powerplant–electrolyzer can be connected via the grid, so the energy used to power the electrolyzer is purchased as a PPA with additional transmission charges. The AEMO ISP 2020, suggests the LCOE of solar and wind farms and the transmission costs for the NEM connected REZs⁴⁵, these range between; US\$22 MWh⁻¹ (A\$30 MWh⁻¹) to US\$29 MWh⁻¹ (A\$40 MWh⁻¹) for Solar LCOE and similarly for Wind LCOE, the costs range US\$23 MWh⁻¹ (A\$32 MWh⁻¹) to US\$50 MWh⁻¹ (A\$70 MWh⁻¹) for Solar LCOE both with additional transmission cost of US\$3.5 MWh⁻¹ (A\$5 MWh⁻¹) to US\$21 MWh⁻¹ (A\$30 MWh⁻¹). However, these network charges could be as high as US\$200 MWh⁻¹ (A\$286 MWh⁻¹) based on tariffs suggested by Australian power suppliers (refer to Supplementary Table 6). These costs can then increase the LC_{H2} by upto between 3 and 4 folds with 70% of the LC_{H2} just contributed by the cost of buying electricity

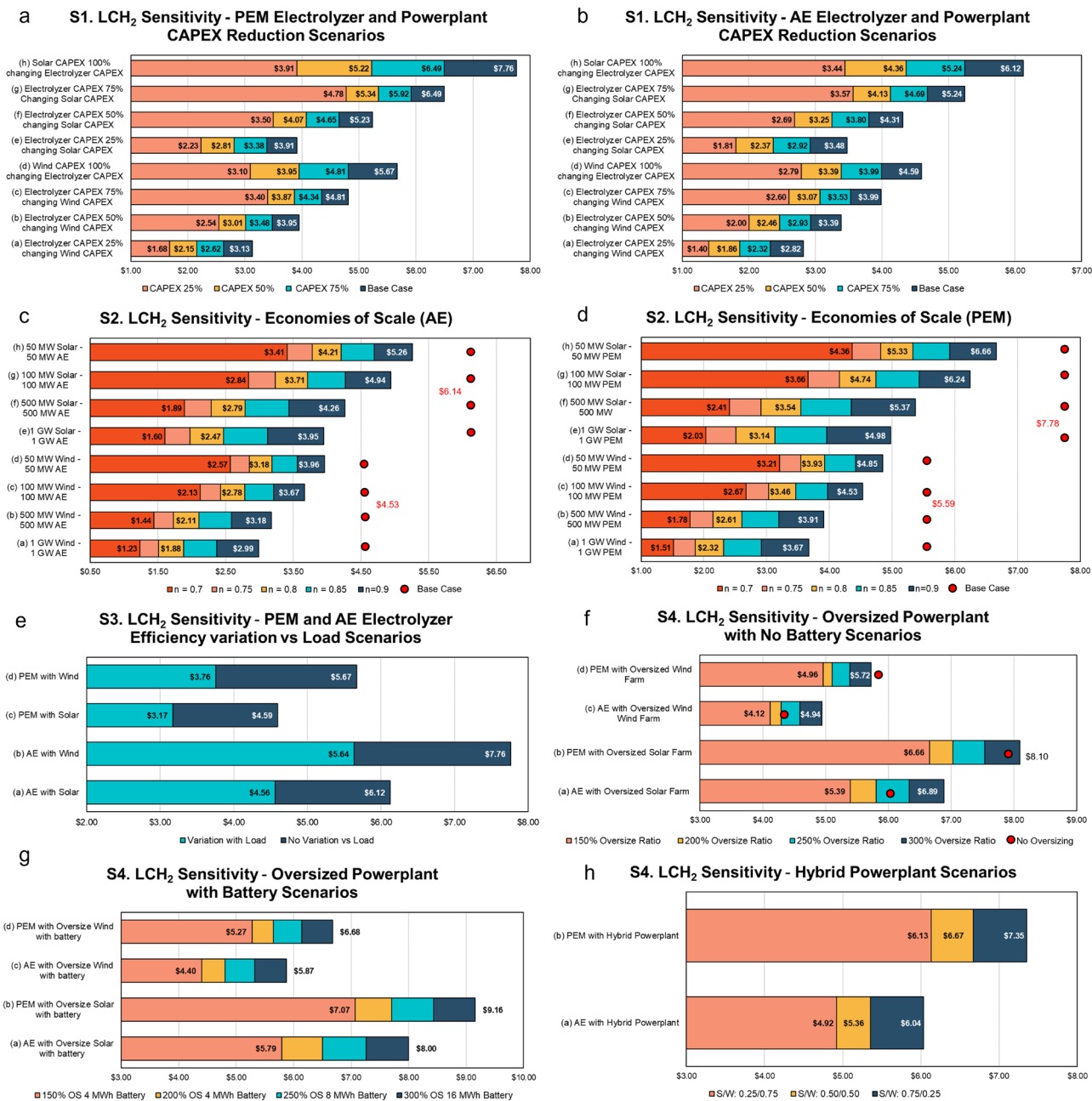


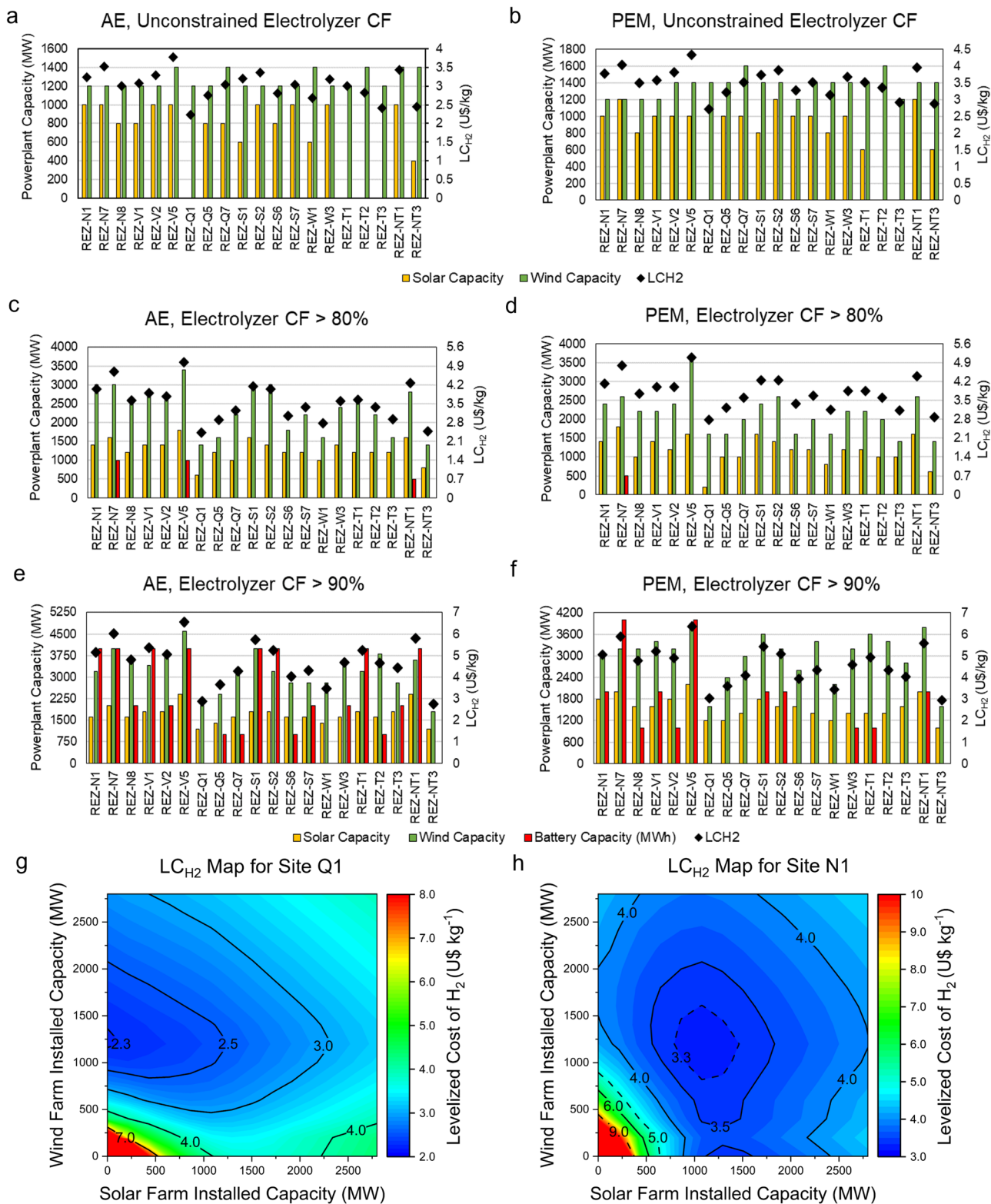
Fig. 5 Sensitivity analysis results. The sensitivity was conducted for the scenarios; S1—capital cost reduction for both **a** AE and **b** PEM electrolyzer system and the powerplant, S2—economies of scale for both **c** AE and **d** PEM system as well as the powerplant, **e** S3—efficiency variation vs load for both class of electrolyzers and S4—electrolyzer and powerplant designs with **f** oversized powerplants without BESS, **g** oversized powerplants with BESS, and **h** hybrid powerplants with varying share of solar and wind for both AE and PEM systems respectively. These scenarios are elaborated in Supplementary Table 8 with base case cost assumptions adapted from Supplementary Table 7. Additional results for categories S3—efficiency improvement and S4—electrolyzer and powerplant design scenarios, that are not represented here are grouped in Supplementary Fig. 18. Here the solar and wind traces of Geraldton was used as an example representation. Note the values are all in US\$.

from the grid. However, connecting the powerplant–electrolyzer has an advantage that the any excess energy (not used by electrolyzer or charge the BESS) can be retailed to the grid, especially if the project proponents can risk selling at the spot prices, the excess can be retailed for upto US\$3500 MWh⁻¹ (A\$5000 MWh⁻¹) based on the highest end spot price in the NEM over 2020⁴⁶, this could potentially offset the transmission costs while yielding additional revenue generation ultimately reducing the LC_{H₂}.

Additional cost reduction can also be generated by retailing the O₂ but this has a very little value due to current low cost of O₂¹⁶, however considering the purity of the O₂ if a suitable offtake

market is available in close proximity a higher retail cost could be achieved.

In this manner, the application of the proposed MCA and cost tool allow an integrated one stop solution for the user to systematically visualize, understand, quantify, and explore different trade-offs between key design aspects and cost parameters and their eventual influence on the overall economics. The results show that several of these parameters play a critical role in driving costs and optimum setting (one or more combinations) for each needs to be matched to achieve the desired costs and performance targets. This is where the next



aspect of the framework, the optimization tool (detailed in next section) brings value as it can identify the right mix of costs and capacity mixes required.

Best case scenario results—application of python algorithm. For the final part of the analysis, the best-case scenario algorithm (refer to Supplementary Note 10) was used to find the standalone powerplant (that can be oversized, made into a hybrid

combination, and complemented with a BESS) and electrolyzer capacity mixes required to achieve the lowest LC_{H2}, with and without constraints on the electrolyzer capacity factor. Initially, the algorithm was run to establish the least LC_{H2} for a maximum of 1 GW electrolyzer capacity with no minimum capacity factor constraint and using the cost/performance parameters (refer to Methods), to provide an overview of the costs that can be achieved. The results for both AE and PEM systems are shown in Fig. 6a, b. As expected, the results (LC_{H2} and capacity mixes) have

Fig. 6 Best Case Scenario Results. The powerplant and BESS capacities required and their subsequent LC_{H_2} to achieve the least cost (unconstrained capacity factor) for both **a** AE and **b** PEM systems, capacity factor target of 80% for both **c** AE and **d** PEM systems and capacity factor target of 90% for both **e** AE and **f** PEM systems are shown for 1 GW electrolyzer capacity. The sites shown here correspond to sites with the best and worst monthly capacity factor variations as in Fig. 4 (The rest of the locations are shown in the Supplementary Figs. 20–21). The contour maps demonstrate the possible LC_{H_2} ranges for 1 GW electrolyzer operated with a mix of Solar and Wind Farms (0–3000 MW each) mapped for 2 sites, **g** site Q1 (Far North Queensland REZ) which is a wind dominant site—a fact supported by the results as the lowest costs (US\$2.3 kg^{-1} –US\$2.5 kg^{-1}) are along the y-axis, and **h** N1 (North West NSW REZ) which is a solar dominant site as reflected by the cost results that show the lowest cost along x-axis (US\$3–3.5 kg^{-1}), moreover the map also shows that similar cost (in the middle of the map) through a hybrid combination with wind (solar capacity 250–2000 MW and wind farm capacity of 750–1750 MW, i.e., $\alpha = 25\%$ –53% and $\beta = 75\%$ –47%). These contour maps highlight that several configurations can get you to within US\$0.5–1 kg^{-1} of the target costs (Australian Target of A\$2 kg^{-1} /US\$1.4 kg^{-1}).

a strong locational dependence due to differing solar and wind profiles. It is observed that for the current CAPEX and OPEX expectations, we can achieve LC_{H_2} of between US\$2.2 kg^{-1} and US\$4.3 kg^{-1} across all sites, with a minimum of US\$2.2 kg^{-1} (AE) and US\$2.7 kg^{-1} (PEM) achieved in REZ-Q1 (Far North Queensland). Comparing both types of electrolyzer highlights that for PEM systems the optimal powerplant configuration differed only slightly from the AE electrolyzer despite having a larger CAPEX than AE, which is countered by their higher load range (assumed minimum load rating of 5% compared to 15% for AE) leading to better capital efficiencies. Therefore, the LC_{H_2} for PEM systems was on average US\$0.5 kg^{-1} higher across all REZs. To achieve these costs, for most of the considered sites, a hybrid powerplant was found to be the best option albeit with different solar and wind shares (α and β ratios—subjective to the local traces). For five of the considered REZs (Q1, T1, T2, T3, and NT3) a wind-only powerplant was found to be best. This tended to be locations with a very strong and consistent wind resource, hence where it was more beneficial to oversize the wind powerplant rather than add solar generation. In addition, the optimum average powerplant oversize ratio was determined to be two times the capacity of the electrolyzer and without the constraint on capacity factor, the BESS is never required since it adds insufficient value to counter the additional high costs it adds to the project.

Comparing the best-case costs to the base case shows typical cost reductions of 50% (mainly due to economies of scale and optimum combination of solar/wind). The comparison reveals similar outcomes, for example, REZ-Q1 was found to have the highest wind potential overall and the lowest solar potential in QLD. In the base case it had the lowest LC_{H_2} of all sites for wind-only and was on par with the average for solar-only for both AE and PEM. For an AE system, the LC_{H_2} for the base case was US\$3.73 kg^{-1} compared to US\$2.24 kg^{-1} for the best-case. For REZ-NT3, optimizing the configuration decreased the levelized cost by 40% compared to the lowest cost in the base case (AE, wind only). In general, the configuration with a hybrid solar and wind powerplant performed better than either on their own, and larger systems had lower levelized costs due to the economies of scale (which is also supported by the sensitivity analysis—Fig. 6). Note, because the scale models which we have incorporated are unconstrained, building a higher capacity will lead to greater cost reductions. To demonstrate this, we used the tool to estimate the LC_{H_2} at a higher scale (>10 GW), the results show that the optimal powerplant remains constant as a ratio of the electrolyzer size. In practice, such scales, certainly at an early stage of industry development would be constrained by the available capital, resources, land, and manufacturing capacity, and put very large amounts of capital at risk. At present, we still have limited data on how costs of mega-scale electrolyzer projects (>100 MW) might scale as such projects are yet to be implemented.

In addition, the minimum electrolyzer CF constraint was included to allow us to model scenarios with greater utilization of

the electrolyzer. Such a requirement might be imposed, for example, by downstream conversion processes. Since for these standalone systems the electrolyzer operating level is driven by the renewable energy available in each timestep, higher capacity factors are achieved by increasing the oversize ratio or adding a BESS into the system to shift excess generation to low-production times. Thus, addition of BESS generally increases the LC_{H_2} compared to the unconstrained case. Setting the minimum electrolyzer capacity factor over the year to 80% increased the average cost across all the sites to \$3.73 kg^{-1} (Fig. 6c, d). All sites relied on a hybrid solar and wind powerplant to achieve this capacity factor since this greatly increases the time that the electrolyzer can operate due to their complementary nature. Despite the lower capital and operating costs of the solar plant, all the sites had a higher share of wind capacity than solar capacity (on average $\alpha = 35\%$ and $\beta = 65\%$) in the combined hybrid powerplant capacity, likely because the wind farms have a higher capacity factor. Although only one of the considered sites (REZ-N7) needed a BESS to meet this target, the powerplant oversize ratio is also much higher than the unconstrained scenario at around 3.23.

To achieve an electrolyzer capacity factor of 90% over the year, BESS were required in the configuration for 11 out of the 20 REZs shown in Fig. 6e, f. The average LC_{H_2} increased to US\$4.45 kg^{-1} and the average powerplant oversize was 4.5, hence involving periods of very high spill. Note that for the BESS, there is an interplay between the BESS power capacity (MW) and the duration of storage that needs to be considered when finding the minimum cost as shown in the sensitivity analysis. Such analysis falls outside the scope of this work but can be explored at a later stage using our tool. Interestingly, for some sites the costs does not vary much by constraining the capacity factors, this could be explained by several factors like (i) as found in our earlier work there is an optimum oversize ratio which despite increase of solar/wind capacity and their cost leads to lower LC_{H_2} , (ii) achieving an 80% capacity factor leads to higher capital efficiencies of the electrolyzer and the increase in costs are countered by higher hydrogen production or (iii) by chance at the site the capacity mix for achieving the least LC_{H_2} is same or close to that to achieve the capacity factor constraints. For reference, the electrolyzer capacity factor in the unconstrained case was between 50% and 76% for AE and 58% and 81% for PEM. This is much higher than the base case because of the power plant oversizing. While we do not map these, like the LC_{H_2} case there are ranges of powerplant configurations which would result in similar capacity factors being achieved.

The best-case algorithm also allows us to visualize the solution space as two of the inputs are changed. As in the contour graphs in Fig. 6g, h, which maps the LC_{H_2} as a function of solar and wind capacity for a constant electrolyzer size, we can see that though the minimal value is reached only once, there are ranges of powerplant configurations which will result in similar levelized costs. We also ran the results for future capital cost reduction (refer to Supplementary Fig. 19) and see that under current economies of scale assumptions at 1 GW scale at 50% reduction

in reference capital cost of electrolyzer and the powerplant (solar/wind) will lead to some sites achieving the US\$1.4 kg⁻¹ (the Australian target of A\$2 kg⁻¹) and at 50–100 GW this is achievable for more sites.

Conclusion

We have developed a comprehensive framework for preliminary design and prefeasibility analysis of exclusively solar and wind powered electrolysis. The framework consists of zoning filters, a multi criteria analysis, a comprehensive cost analysis tool and a best-case scenario algorithm. While such tools/frameworks have been developed before, our system provides an integrated framework tools and functionalities that can then be used individually and ideally altogether to optimize across the stages of renewable electrolysis project design which is missing in prior work. We apply this framework to the emerging Australian Hydrogen market as a case study, by identifying and comparing 41 different sites across the country for potential hydrogen hubs. This extends to evaluating each site's solar and wind potential, locational viability (water resource, proximity to end use application etc.) and levelised cost of generating hydrogen. The cost tool is then used to understand the influence of local renewable energy potential (local solar and wind resource), different design parameters (oversizing, hybrid combination, BESS storage, grid connection etc.), cost (economies of scale) and performance parameters (degradation rates, efficiency variation with load etc.). Subsequently the best-case scenario algorithm is applied to individual sites to determine installed capacities of electrolyzer, solar/wind powerplant and BESS capacity to achieve least cost or target capacity factors. Our MCA results show that some of the more favourable sites for developing hydrogen projects are in New South Wales, South Australia, Western Australia, and Queensland (subjective to the MCA assumptions). Furthermore, under current cost expectations at 10 MW (scale of existing projects in Australia) the cost of H₂ ranges between US\$6 kg⁻¹ and US\$10 kg⁻¹ (A\$8 kg⁻¹ and A\$14 kg⁻¹). However, scaling up of project capacities to take advantage of economies of scale, optimizing the capacity mixes of the powerplant (oversized Solar/Wind Farm and BESS hybrids) and leveraging the trends for capital cost reduction, can lead to achievement of the Australian target of US\$1.4 kg⁻¹ (A\$2 kg⁻¹) at some favourable sites in the near term (within 10 years) and rest of the sites over the long term. Note while these selected sites are just used as a case study and an indicative representation of each state's hydrogen generation potential as a platform for developing Australia's hydrogen future, the framework can be used to evaluate and identify additional sites not only in Australia as well as in other jurisdictions. To this end, this framework of tools is made available as an open-source resource to assist global development of green hydrogen projects, by providing the user provided the options; to change the weighting, scoring matrix and zoning filters of the MCA tool (currently the tool, that is provided as Supplementary Software 1, is set to our opinion based on consultation with industrial stakeholders), provide the renewable energy data for their jurisdictions and update the techno-economic parameters to match project scope.

Methods

The method section provides the details on the guidelines for collecting data for zoning potential sites, methodology for assessing the renewable energy potential, data collection and scoring guidelines of the MCA tool and the technoeconomic analysis conducted.

Renewable energy zones. The Australian Energy Market Operator (AEMO), as part of its 2020 Integrated System Plan for the National Electricity Market (NEM) has identified 35 REZs across the five NEM States - Queensland (QLD/Q), New South Wales (NSW/N), Victoria (VIC/V), South Australia (SA/S) and Tasmania (TAS/T)⁴⁵. While the ISP does not specify SEZs for Western Australia (WA/W) and Northern Territory (NT) as they are not part of the NEM, the State and Territory Governments have, with industry, identified particularly promising locations for hydrogen projects based on renewable energy potential and available infrastructure. In our study we consider Geraldton, Port Hedland and Ashburton regions in Western Australia as they are already attracting interest as potential specialized zones for green electrolyzer projects to generate hydrogen and its subsequent conversion to ammonia as a means for renewable energy export^{47–49}. Similarly, in the Northern Territory, locations including Baines, McArthur, and Tennant Creek have high renewable energy generation potential. Tennant Creek's potential for renewable hydrogen production has already been acknowledged, with a trial off-grid hydrogen project to be implemented in 2021⁵⁰. Tennant Creek also neighbours the town of Elliot, where the Sun Cable project to export solar energy to Singapore via HVDC cable is being developed⁵¹. Other considerations for these site selections for NT and WA were their proximity to highways, railways, existing gas pipelines and ports. A similar preliminary analysis by Geoscience Australia also finds these regions to be amongst the high to moderately suitable locations for hydrogen generation⁵². We provide a comparative analysis of all these REZ and additional selected locations to assess Australia's renewable hydrogen generation potential.

Water availability. For this analysis, we consider locations close to the coast where water can be sourced through desalination plants, while inland locations will need access to either fresh water, underground aquifers, desalination plants or recycled water (refer to Supplementary Figs. 1–3). For costing these choices, we consider wholesale prices of fresh water, recycled water, and desalinated water as A\$2.5 kL⁻¹, A\$1.6 kL⁻¹ and A\$2.5 kL⁻¹ respectively, based on typical wholesale water supply prices in Australia (refer to Supplementary Table 1).

Downstream utilization opportunities. For export opportunities, we consider findings in a study by ARUP that identified ports that are suitable for hosting export facilities for hydrogen and its derivatives (refer to Supplementary Table 3)⁴⁹. For local demand, we identify demand centres which include ammonia production facilities, cement plants, steel making plants etc. where hydrogen can be used for decarbonisation. Moreover, we identify other distributed applications like use of hydrogen for mobility application at mines, injection in natural gas pipelines, storage of renewable energy for electricity generation or for replacement of diesel/natural gas-based energy generators in off grid locations. The details of these opportunities for each REZ are highlighted in Supplementary Data 2. Note we do not assess the technical and economic feasibility of these opportunities, however, use them as a metric to compare the potential of different REZs to host hydrogen hubs using the MCA.

Additional support infrastructure. To identify potential underground H₂ storage opportunities we consider salt caverns and depleting oil/natural gas fields that have been identified as part of a technical analysis conducted by CSIRO for identifying suitable sites for large scale underground hydrogen storage (refer to Supplementary Fig. 13)⁵³. Similarly for transport network, electricity grid and natural gas network, we consider existing road and railway lines, power transmission lines and natural gas pipelines. Note similar to utilization, we do not assess the technical and economic feasibility of leveraging these resources, however, use them as a metric to compare the potential of different REZs to host hydrogen hubs using the MCA.

Renewable energy availability

Solar and wind profiles. As elaborated earlier, our cost tool relies on time-sequential, hourly observations of the solar and wind data at each location to assess its power generation potential. The tool comes preloaded with solar/wind traces (hourly data over a year) for 41 locations across Australia and allows users to add their own custom solar/wind profiles as well. We obtain these solar and wind traces from publicly available databases: the AEMO ISP 2020 Database and the Open-Source tool "Renewables Ninja" (refer to Supplementary Note 3). Note there are differences in base line assumptions in both models, the Renewables Ninja model considers a 10% power loss due to conversion loss for solar (DC to AC conversion⁵⁴) while the AEMO ISP assume the solar plant are practically inherently oversized to counter this energy loss (DC to AC ratio is assumed to be between 1.1 and 1.3 to counter the energy loss⁵⁵). Similarly, the AEMO ISP assumes a 10% loss in energy output for wind which can be attributed to the interaction of wind turbines resulting in loss of area and interference in wind patterns⁵⁶, while the Renewables Ninja does not consider this. For consistency we consider a correction factor of 1.11 and 0.9 for solar and wind traces respectively, for the raw data extracted from renewable ninja to counter the above discrepancies in between the two databases.

The data from both resources was extracted and resampled to an hourly format and is already preloaded in the tool. The tool then correlates the hourly

Table 2 The MCA framework weighting and scoring rules.

Category	Weight	Justification
Renewable energy potential	40%	Achieving high-capacity operation is a key target for our analysis and comparison between each site. The location viability would act as a differentiator between sites with similar renewable energy potential and is equally important economically and operationally as capacity factors. Sites which can leverage existing or easy to tap resources/ infrastructure are at a higher advantage than those that cannot. Finding suitable end use of hydrogen is also critical for project development, while we do not particularly explore individual end use opportunities in detail. We identify some key opportunities that could be tapped. The category currently includes bulk storage opportunities which are highly distributed across Australia, therefore might not be applicable to all locations, but would provide additional advantage to the locations selected in proximity.
Location viability	30%	
End use opportunity	20%	
Storage opportunity	10%	
Scores	Qualitative score	Quantitative score
Renewable energy potential		
1. Capacity factor		
— Solar	+5	>30% +0
— Wind	+5	>50% +0
2. Variability (S.D. is standard deviation)		
— Solar	+5	30–27.5% -1
— Wind	+5	50–45% -1
		27.5– 25% -2
		45–40% -2
		5% ≤ S.D. < 6% -1
		6% ≤ S.D. < 7% -1
		7% ≤ S.D. < 8% -2
		8% ≤ S.D. < 9% -2
		9% ≤ S.D. < 10% -2
		10% ≤ S.D. < 11% -2
		11% ≤ S.D. < 12% -2
		12% ≤ S.D. < 13% -2
		13% ≤ S.D. < 14% -2
		14% ≤ S.D. < 15% -2
		15% ≤ S.D. < 16% -2
		16% ≤ S.D. < 17% -2
		17% ≤ S.D. < 18% -2
		18% ≤ S.D. < 19% -2
		19% ≤ S.D. < 20% -2
		20% ≤ S.D. < 21% -2
		21% ≤ S.D. < 22% -2
		22% ≤ S.D. < 23% -2
		23% ≤ S.D. < 24% -2
		24% ≤ S.D. < 25% -2
		25–20% -3
		40–35% -3
		6% ≤ S.D. < 7% -3
		7% ≤ S.D. < 8% -3
		8% ≤ S.D. < 9% -3
		9% ≤ S.D. < 10% -3
		10% ≤ S.D. < 11% -3
		11% ≤ S.D. < 12% -3
		12% ≤ S.D. < 13% -3
		13% ≤ S.D. < 14% -3
		14% ≤ S.D. < 15% -3
		15% ≤ S.D. < 16% -3
		16% ≤ S.D. < 17% -3
		17% ≤ S.D. < 18% -3
		18% ≤ S.D. < 19% -3
		19% ≤ S.D. < 20% -3
		20% ≤ S.D. < 21% -3
		21% ≤ S.D. < 22% -3
		22% ≤ S.D. < 23% -3
		23% ≤ S.D. < 24% -3
		24% ≤ S.D. < 25% -3
		25–20% -3
		40–35% -3
		6% ≤ S.D. < 7% -3
		7% ≤ S.D. < 8% -3
		8% ≤ S.D. < 9% -3
		9% ≤ S.D. < 10% -3
		10% ≤ S.D. < 11% -3
		11% ≤ S.D. < 12% -3
		12% ≤ S.D. < 13% -3
		13% ≤ S.D. < 14% -3
		14% ≤ S.D. < 15% -3
		15% ≤ S.D. < 16% -3
		16% ≤ S.D. < 17% -3
		17% ≤ S.D. < 18% -3
		18% ≤ S.D. < 19% -3
		19% ≤ S.D. < 20% -3
		20% ≤ S.D. < 21% -3
		21% ≤ S.D. < 22% -3
		22% ≤ S.D. < 23% -3
		23% ≤ S.D. < 24% -3
		24% ≤ S.D. < 25% -3
		25–20% -3
		40–35% -3
		6% ≤ S.D. < 7% -3
		7% ≤ S.D. < 8% -3
		8% ≤ S.D. < 9% -3
		9% ≤ S.D. < 10% -3
		10% ≤ S.D. < 11% -3
		11% ≤ S.D. < 12% -3
		12% ≤ S.D. < 13% -3
		13% ≤ S.D. < 14% -3
		14% ≤ S.D. < 15% -3
		15% ≤ S.D. < 16% -3
		16% ≤ S.D. < 17% -3
		17% ≤ S.D. < 18% -3
		18% ≤ S.D. < 19% -3
		19% ≤ S.D. < 20% -3
		20% ≤ S.D. < 21% -3
		21% ≤ S.D. < 22% -3
		22% ≤ S.D. < 23% -3
		23% ≤ S.D. < 24% -3
		24% ≤ S.D. < 25% -3
		25–20% -3
		40–35% -3
		6% ≤ S.D. < 7% -3
		7% ≤ S.D. < 8% -3
		8% ≤ S.D. < 9% -3
		9% ≤ S.D. < 10% -3
		10% ≤ S.D. < 11% -3
		11% ≤ S.D. < 12% -3
		12% ≤ S.D. < 13% -3
		13% ≤ S.D. < 14% -3
		14% ≤ S.D. < 15% -3
		15% ≤ S.D. < 16% -3
		16% ≤ S.D. < 17% -3
		17% ≤ S.D. < 18% -3
		18% ≤ S.D. < 19% -3
		19% ≤ S.D. < 20% -3
		20% ≤ S.D. < 21% -3
		21% ≤ S.D. < 22% -3
		22% ≤ S.D. < 23% -3
		23% ≤ S.D. < 24% -3
		24% ≤ S.D. < 25% -3
		25–20% -3
		40–35% -3
		6% ≤ S.D. < 7% -3
		7% ≤ S.D. < 8% -3
		8% ≤ S.D. < 9% -3
		9% ≤ S.D. < 10% -3
		10% ≤ S.D. < 11% -3
		11% ≤ S.D. < 12% -3
		12% ≤ S.D. < 13% -3
		13% ≤ S.D. < 14% -3
		14% ≤ S.D. < 15% -3
		15% ≤ S.D. < 16% -3
		16% ≤ S.D. < 17% -3
		17% ≤ S.D. < 18% -3
		18% ≤ S.D. < 19% -3
		19% ≤ S.D. < 20% -3
		20% ≤ S.D. < 21% -3
		21% ≤ S.D. < 22% -3
		22% ≤ S.D. < 23% -3
		23% ≤ S.D. < 24% -3
		24% ≤ S.D. < 25% -3
		25–20% -3
		40–35% -3
		6% ≤ S.D. < 7% -3
		7% ≤ S.D. < 8% -3
		8% ≤ S.D. < 9% -3
		9% ≤ S.D. < 10% -3
		10% ≤ S.D. < 11% -3
		11% ≤ S.D. < 12% -3
		12% ≤ S.D. < 13% -3
		13% ≤ S.D. < 14% -3
		14% ≤ S.D. < 15% -3
		15% ≤ S.D. < 16% -3
		16% ≤ S.D. < 17% -3
		17% ≤ S.D. < 18% -3
		18% ≤ S.D. < 19% -3
		19% ≤ S.D. < 20% -3
		20% ≤ S.D. < 21% -3
		21% ≤ S.D. < 22% -3
		22% ≤ S.D. < 23% -3
		23% ≤ S.D. < 24% -3
		24% ≤ S.D. < 25% -3
		25–20% -3
		40–35% -3
		6% ≤ S.D. < 7% -3
		7% ≤ S.D. < 8% -3
		8% ≤ S.D. < 9% -3
		9% ≤ S.D. < 10% -3
		10% ≤ S.D. < 11% -3
		11% ≤ S.D. < 12% -3
		12% ≤ S.D. < 13% -3
		13% ≤ S.D. < 14% -3
		14% ≤ S.D. < 15% -3
		15% ≤ S.D. < 16% -3
		16% ≤ S.D. < 17% -3
		17% ≤ S.D. < 18% -3
		18% ≤ S.D. < 19% -3
		19% ≤ S.D. < 20% -3
		20% ≤ S.D. < 21% -3
		21% ≤ S.D. < 22% -3
		22% ≤ S.D. < 23% -3
		23% ≤ S.D. < 24% -3
		24% ≤ S.D. < 25% -3
		25–20% -3
		40–35% -3
		6% ≤ S.D. < 7% -3
		7% ≤ S.D. < 8% -3
		8% ≤ S.D. < 9% -3
		9% ≤ S.D. < 10% -3
		10% ≤ S.D. < 11% -3
		11% ≤ S.D. < 12% -3
		12% ≤ S.D. < 13% -3
		13% ≤ S.D. < 14% -3
		14% ≤ S.D. < 15% -3
		15% ≤ S.D. < 16% -3
		16% ≤ S.D. < 17% -3
		17% ≤ S.D. < 18% -3
		18% ≤ S.D. < 19% -3
		19% ≤ S.D. < 20% -3
		20% ≤ S.D. < 21% -3
		21% ≤ S.D. < 22% -3
		22% ≤ S.D. < 23% -3
		23% ≤ S.D. < 24% -3
		24% ≤ S.D. < 25% -3
		25–20% -3
		40–35% -3
		6% ≤ S.D. < 7% -3
		7% ≤ S.D. < 8% -3
		8% ≤ S.D. < 9% -3
		9% ≤ S.D. < 10% -3
		10% ≤ S.D. < 11% -3
		11% ≤ S.D. < 12% -3
		12% ≤ S.D. < 13% -3
		13% ≤ S.D. < 14% -3
		14% ≤ S.D. < 15% -3
		15% ≤ S.D. < 16% -3
		16% ≤ S.D. < 17% -3
		17% ≤ S.D. < 18% -3
		18% ≤ S.D. < 19% -3
		19% ≤ S.D. < 20% -3
		20% ≤ S.D. < 21% -3
		21% ≤ S.D. < 22% -3
		22% ≤ S.D. < 23% -3
		23% ≤ S.D. < 24% -3
		24% ≤ S.D. < 25% -3
		25–20% -3
		40–35% -3
		6% ≤ S.D. < 7% -3
		7% ≤ S.D. < 8% -3
		8% ≤ S.D. < 9% -3
		9% ≤ S.D. < 10% -3
		10% ≤ S.D. < 11% -3
		11% ≤ S.D. < 12% -3
		12% ≤ S.D. < 13% -3
		13% ≤ S.D. < 14% -3
		14% ≤ S.D. < 15% -3
		15% ≤ S.D. < 16% -3
		16% ≤ S.D. < 17% -3
		17% ≤ S.D. < 18% -3
		18% ≤ S.D. < 19% -3
		19% ≤ S.D. < 20% -3
		20% ≤ S.D. < 21% -3
		21% ≤ S.D. < 22% -3
		22% ≤ S.D. < 23% -3
		23% ≤ S.D. < 24% -3
		24% ≤ S.D. < 25% -3
		25–20% -3
		40–35% -3
		6% ≤ S.D. < 7% -3
		7% ≤ S.D. < 8% -3
		8% ≤ S.D. < 9% -3
		9% ≤ S.D. < 10% -3
		10% ≤ S.D. < 11% -3
		11% ≤ S.D. < 12% -3
		12% ≤ S.D. < 13% -3
		13% ≤ S.D. < 14% -3
		14% ≤ S.D. < 15% -3
		15% ≤ S.D. < 16% -3
		16% ≤ S.D. < 17% -3
		17% ≤ S.D. < 18% -3
		18% ≤ S.D. < 19% -3
		19% ≤ S.D. < 20% -3
		20% ≤ S.D. < 21% -3
		21% ≤ S.D. < 22% -3
		22% ≤ S.D. < 23% -3
		23% ≤ S.D. < 24% -3
		24% ≤ S.D. < 25% -3
		25–20% -3
		40–35% -3
		6% ≤ S.D. < 7% -3
		7% ≤ S.D. < 8% -3
		8% ≤ S.D. < 9% -3
		9% ≤ S.D. < 10% -3
		10% ≤ S.D. < 11% -3
		11% ≤ S.D. < 12% -3
		12% ≤ S.D. < 13% -3
		13% ≤ S.D. < 14% -3
		14% ≤ S.D. < 15% -3
		15% ≤ S.D. < 16% -3
		16% ≤ S.D. < 17% -3
		17% ≤ S.D. < 18% -3
		18% ≤ S.D. < 19% -3
		19% ≤ S.D. < 20% -3
		20% ≤ S.D. < 21% -3
		21% ≤ S.D. < 22% -3
		22% ≤ S.D. < 23% -3
		23% ≤ S.D. < 24% -3
		24% ≤ S.D. < 25% -3
		25–20% -3
		40–35% -3
		6% ≤ S.D. < 7% -3
		7% ≤ S.D. < 8% -3
		8% ≤ S.D. < 9% -3
		9% ≤ S.D. < 10% -3
		10% ≤ S.D. < 11% -3
		11% ≤ S.D. < 12% -3
		12% ≤ S.D. < 13% -3
		13% ≤ S.D. < 14% -3

Table 3 Input ranges considered for the best performance analysis.

Parameter	Range	Step change
Electrolyzer capacity (MW _{elec})	100–1000	100
Solar farm capacity (MW _{SolarFarm} /MW _{elec})	0–4	0.2
Wind farm capacity (MW _{WindFarm} /MW _{elec})	0–4	0.2
BESS power (MW _{BESS} /MW _{elec})	0–2	0.5
BESS storage duration (hours)	1, 2, 4 and 8	NA
Cost and performance parameters	Adopted from Supplementary Table 7	25–75% reduction in CAPEX Considered

generation data with the specific energy consumption of the electrolyzer to model the hydrogen generated, also on an hourly basis. This hourly data can then be represented as a sorted annual distribution of the power output from the solar PV or the wind powerplant, or as power consumed by the electrolyzer, using a similar protocol detailed in our prior analysis¹⁶.

Moreover, these duration curves were arranged as (i) an annual duration curve (refer to Supplementary Figs. 4–5) which shows the total energy output by the powerplant, i.e., the area under the duration curve and the total time that the power output is maintained at any particular proportion of the capacity of the powerplant, and (ii) as the monthly distribution curve (refer to Fig. 4 and Supplementary Figs. 6–11) which show the maximum/minimum capacity factor, the standard deviation in capacity factors (the normal standard deviation and \pm standard deviation) and average capacity factors. It is assumed that these solar/wind profiles are independent of the size of the powerplant, and thus apply to any scale.

Renewable potential assessment. To evaluate and compare the renewable energy potential, we use the capacity factor and seasonal variability as key metrics, as elaborated below:

Capacity factor: The capacity factor of the powerplant achieved over the year at each site is evaluated as shown in Eq. 2:

$$C_{F,x} = \frac{\text{Actual Energy Output}(E_x)}{\text{Theoretical Maximum Energy Output}(E_{O,x})} \quad (2)$$

Here E_x represents the area under the annual duration curve. We also consider hybrid powerplant options, i.e., a combination of solar and wind farm within the same REZ to drive the electrolyzer. To model the performance of the hybrid system, the hourly wind and solar capacity factors (C_F) are added as a weighted sum with the respective weightings defined by the hybrid ratio as shown in Eq. 3:

$$C_{F,h}(t) = \alpha \times C_{F,s}(t) + \beta \times C_{F,w}(t) \quad (3)$$

Here $C_{F,h}(t)$ is the capacity factor of the hybrid system at any given time, $C_{F,s}(t)$ and $C_{F,w}(t)$ are the capacity factor of the individual solar PV and wind farms, respectively, while α is the percentage of the solar PV and β is the percentage of the wind farm in the total capacity of the hybrid system ($\beta = 1 - \alpha$). E.g., if there is a 10 MW hybrid powerplant with 7 MW solar and 3 MW wind then $\alpha = 70\%$ and $\beta = 30\%$. Moreover, $C_{F,h}(t)$ can be subsequently converted into the duration curves of the hybrid powerplant. In configurations including a BESS Energy Storage System (BESS), the additional power stored in the BESS is included as part of the overall capacity factor of the renewable generator and electrolyzer.

Seasonal variability: To quantify the seasonal variability, we assess the standard deviation of the average monthly capacity factors across the year for each state, with the sites with the higher standard deviations are more susceptible to seasonal variability. For the monthly duration curves (refer to Fig. 4 and Supplementary Figs. 6–11), the seasonal variability is elaborated in more detail using metrics like average monthly capacity factor, the standard deviation of the capacity factors in the month and the maximum/minimum capacity factors achieved over each month of the year.

Multi criteria analysis

MCA database. To build the MCA database, a comprehensive analysis of all the MCA categories was conducted for each REZ based on the defined zoning filters. The data is presented in Supplementary Data 2.

MCA weighting and scores. The MCA provides a score out of 10 for each REZ depending on weighting of each category as well as their constituent qualitative and quantitative scores. The reference score ranges for these qualitative/quantitative measures and the subsequent scores for each site in each category were then assigned based on sample data collected from the location (refer to Supplementary Data 2). The scoring scheme we consider herein is summarized in Table 2 (for additional details refer to Supplementary Note 6). Note the current weighting and scores are based on our assumptions after analyzing different real-life projects and engagement with project proponents, and to accommodate the

changes the user might need to make the resource is provided as an open-source tool which can be altered to reflect the design choices faced by the user. In addition, an editable MCA tool is provided as an excel file with the Supplementary Materials (Supplementary Software 1).

Electrolyzer design configurations. Based on the considered technologies, several representative configurations of the powerplant can be developed, including operating the electrolyzer with just a solar PV or a wind farm or both (hybrid), with or without BESS, and in a standalone or grid connected configuration (refer to Supplementary Note 7). For the BESS system a simple algorithm that causes the BESS to charge when there is excess energy and discharge when there is a deficit was used (refer to Supplementary Note 7). Through our tool, all these options can be assessed at each site, providing detailed comparative analysis of configuration options.

Technoeconomic analysis

Technoeconomic parameters: The technoeconomic parameters considered for the solar PV, wind turbines, BESS and the electrolyzer systems and were compiled from literature based on current and future estimates. These are elaborated in the Supplementary Information (Supplementary Note 8 and Supplementary Tables 6–7).

Economic metrics: Herein, we focus on the levelized cost of hydrogen as the key analysis metric. To evaluate the levelized cost of hydrogen (LC_{H_2}), a standard discounted cash flow was applied over the plant lifetime (n). The key cash flows included the upfront capital costs (assumed to be incurred over year 0, i.e., the construction period), the ongoing annual operating costs and additional product sales (sale of surplus electricity or oxygen) over year i (from year 0 to n), which were discounted to year 0 using a discount rate (r) to establish the net present value. A nominal pre-tax environment was assumed; therefore, no inflation and depreciation were applied to the operating costs/sales and the capital assets, respectively. In this manner, Eq. 4 shows how the LC_{H_2} was calculated.

$$LC_{H_2} = \frac{\sum_{i=0}^n \frac{\text{CAPEX}_i + \text{OPEX}_i - \text{Sales}_i}{(1+r)^i}}{\sum_{i=1}^n \frac{\text{Hydrogen Production}_i}{(1+r)^i}} \quad (4)$$

The levelized cost is calculated in United States Dollars—US\$ (2021 basis) calculated over a 20-year project life using a discount rate of 7%.

Note the HySupply cost tool allows a detailed cash flow statement to evaluate the economic viability of the projects using the payback period, net profit, and the return on investment as metrics (refer to Supplementary Fig. 14).

Best performance analysis. The python-script based “optimization tool” was developed to iteratively step through the possible range of various input parameters and return the set of parameters that give the desired least cost LC_{H_2} and capacity factor development scenario for standalone systems. The script is presented in the Supplementary Information (refer to Supplementary Note 10) and the tool takes as inputs the electrolyzer nominal capacity, the powerplant capacity as a ratio of the electrolyzer capacity (oversize ratio), the ratio of solar to wind contributing to the powerplant (in case of hybrid system), the energy storage system rated power and duration of storage, and the solar/wind profile of the chosen location. The algorithm can also be fed a minimum allowable capacity factor for the annual electrolyzer operation as a proxy for annual hydrogen production. Upper and lower bounds are set on each of the quantitative parameters along with a step size which determines how many possible configurations are tested. The LC_{H_2} calculation is then run for each configuration and the tool returns the set of input parameters (electrolyzer nominal capacity, powerplant capacity, oversize ratio, hybrid ratio, BESS rated power and BESS storage duration) which give the least cost. The inputs used for the analysis are shown in Table 3.

Framework limitations. While we have endeavoured to develop a comprehensive and inclusive assessment framework and tool, they remain work in progress with further developments to address present limitations including:

1. The MCA in its current form is based on our understanding and is subjective to application and interpretation of the users. We are engaging

with hydrogen project proponents and other stakeholders to further enhance the MCA scope. These changes will be included in further iterations, and the MCA is made available as an open-source resource so that users can add their own parameters or adapt the current assumptions to their own requirement.

- The cost tool only allows for exclusive solar/wind powered scenarios and is limited to generation i.e., downstream storage, additional compression requirements and utilization are not considered, as the design for these are subjective to the nature of application and can add considerable complexities. Again, the cost tool is made available to allow users to provide their own inputs, while default values are provided for reference these are based on publicly available data. We are engaging with technology developers to continue improving the tools and updating the defaults to match the current state of the art.
- The best-case scenario algorithm is more simplistic than the cost tool as it is currently only configured to run standalone combinations and does not cater for degradation (of powerplant and electrolyzer) nor electrolyzer efficiency variation with load. These factors and additional functionalities can be added to the script; however, this would increase the number of iterations and time required to achieve the best combination.

Data availability

The authors declare that the data supporting the findings of this study are available within the paper and its supplementary information and supplementary data (<https://doi.org/10.6084/m9.figshare.21529530>).

Code availability

The MCA Tool is attached as an excel sheet is provided as Supplementary Software 1 (or can be accessed at <https://doi.org/10.6084/m9.figshare.21441339>). Similarly, the Python Script for the best scenario algorithm is presented in the supplementary information (the python files can be found at <https://doi.org/10.6084/m9.figshare.21441354>). While the HySupply cost tool is available on the GlobH2e website (<https://www.globh2e.org.au/hysupply-cost-tool>). For the terms and references on the use of these tools please refer to Supplementary Note 10.

Received: 21 July 2022; Accepted: 10 November 2022;

Published online: 06 December 2022

References

- Ueckerdt, F. et al. Potential and risks of hydrogen-based e-fuels in climate change mitigation. *Nat. Clim. Chang.* **11**, 384–393 (2021).
- IEA. *The Future of Hydrogen*. (IEA, 2019).
- IEA. *Net Zero by 2050 - A Roadmap for the Global Energy Sector*. <https://www.iea.org/reports/net-zero-by-2050> (2021).
- IRENA. *Hydrogen: a Renewable Energy Perspective*. (IRENA, 2019).
- Christensen, A. *Assessment of Hydrogen Production Costs from Electrolysis: United States and Europe*. (International Council on Clean Transportation (ICCT), 2020).
- Mansilla, C. et al. Chapter 7 - Hydrogen Applications: Overview of the Key Economic Issues and Perspectives. in (ed. Azzaro-Pantel, C. B. T.-H. S. C.) 271–292 (Academic Press, 2018). <https://doi.org/10.1016/B978-0-12-811197-0.00007-5>.
- IEA. *World Energy Outlook 2021*. <https://www.iea.org/reports/world-energy-outlook-2021> (2021).
- IRENA. *Renewable Power Generation Costs in 2020*. [publications/2020/Jun/Renewable-Power-Costs-in-2019 (2021).
- IRENA. *Green Hydrogen Cost Reduction: Scaling up Electrolysers to Meet the 1.5°C Climate Goal*. (2020).
- Hydrogen Council & McKinsey & Company. *Hydrogen Insights: A perspective on hydrogen investment, market development, and cost competitiveness*. www.hydrogencouncil.com. (2021).
- Bloomberg New Energy Finance. *Hydrogen Economy Outlook*. (2020).
- Kopp, M. et al. Energiepark Mainz: technical and economic analysis of the worldwide largest Power-to-Gas plant with PEM electrolysis. *Int. J. Hydrogen Energy* **42**, 13311–13320 (2017).
- Uusitalo, V., Väisänen, S., Inkeri, E. & Soukka, R. Potential for greenhouse gas emission reductions using surplus electricity in hydrogen, methane and methanol production via electrolysis. *Energy Convers. Manag.* **134**, 125–134 (2017).
- Smith, C., Hill, A. K. & Torrente-Murciano, L. Current and future role of Haber-Bosch ammonia in a carbon-free energy landscape. *Energy Environ. Sci.* **13**, 331–344 (2020).
- Abe, J. O., Popoola, A. P. I., Ajenifuja, E. & Popoola, O. M. Hydrogen energy, economy and storage: Review and recommendation. *Int. J. Hydrogen Energy* **44**, 15072–15086 (2019).
- Ali Khan, M. H. et al. Designing optimal integrated electricity supply configurations for renewable hydrogen generation in Australia. *iScience* **24**, 102539 (2021).
- Al-Sharafi, A., Sahin, A. Z., Ayar, T. & Yilbas, B. S. Techno-economic analysis and optimization of solar and wind energy systems for power generation and hydrogen production in Saudi Arabia. *Renew. Sustain. Energy Rev.* **69**, 33–49 (2017).
- Khalilnejad, A. & Riahy, G. H. A hybrid wind-PV system performance investigation for the purpose of maximum hydrogen production and storage using advanced alkaline electrolyzer. *Energy Convers. Manag.* **80**, 398–406 (2014).
- Akyuz, E., Oktay, Z. & Dincer, I. Performance investigation of hydrogen production from a hybrid wind-PV system. *Int. J. Hydrogen Energy* **37**, 16623–16630 (2012).
- Niaz, H. & Liu, J. J. A Mixed Integer Dynamic Optimization Approach for a Hybrid-Stand Alone Solar and Wind Powered Alkaline Water Electrolyser for Renewable Hydrogen. in *31 European Symposium on Computer Aided Process Engineering* (eds. Turkey, M. & Gani, R. B. T.-C. A. C. E.) vol. 50, 1285–1291 (Elsevier, 2021).
- Kikuchi, Y., Ichikawa, T., Sugiyama, M. & Koyama, M. Battery-assisted low-cost hydrogen production from solar energy: rational target setting for future technology systems. *Int. J. Hydrogen Energy* **44**, 1451–1465 (2019).
- Glenk, G. & Reichelstein, S. Economics of converting renewable power to hydrogen. *Nat. Energy* **4**, 216–222 (2019).
- van Leeuwen, C. & Mulder, M. Power-to-gas in electricity markets dominated by renewables. *Appl. Energy* **232**, 258–272 (2018).
- NREL. H2A: Hydrogen Analysis Production Models. <https://www.nrel.gov/hydrogen/h2a-production-models.html>.
- Ludwig-Bölkow-Systemtechnik GmBH. E3Database - The Life-cycle Assessment Tool. <http://www.e3database.com/>.
- Commonwealth of Australia (Geoscience Australia). AusH2 - Australia's Hydrogen Opportunities Tool. <https://portal.ga.gov.au/persona/hydrogen> (2021).
- Brändle, G., Schönfisch, M. & Schulte, S. *Estimating Long-Term Global Supply Costs for Low-Carbon Hydrogen*. https://www.ewi.uni-koeln.de/cms/wp-content/uploads/2021/03/EWI_WP_20-04_Estimating_long-term_global_supply_costs_for_low-carbon_Schoenfisch_Braendle_Schulte-1.pdf (2020).
- Khrouz, M. et al. Life Cycle Costing Analysis: Tools and Applications for Determining Hydrogen Production Cost for Fuel Cell Vehicle Technology. *Energies* **13** (2020).
- Daiyan, R. et al. *The Case for An Australian Hydrogen Export Market to Germany, State of Play Version 1.0*. <https://doi.org/10.26190/35zd-8p21> (2021).
- Australian Government. *Technology Investment Roadmaps - First Low Emissions Technology Statement 2020*. <https://www.industry.gov.au/data-and-publications/technology-investment-roadmap-first-low-emissions-technology-statement-2020> (2020).
- CSIRO. Australia. *HyResource* <https://research.csiro.au/hyresource/policy/australia-and-new-zealand/australia/> (2021).
- Daiyan, R. et al. *The Case for an Australian Hydrogen Export Market to Germany: State of Play Working paper for consultation*. (UNSW Sydney, 2021). <https://doi.org/10.26190/35zd-8p21>.
- Nagashima, M. *Japan's Hydrogen Strategy and Its Economic and Geopolitical Implications*. (2018).
- Ha, J. E. Hydrogen Economy Plan in Korea Current situation in Korea Aiming High. 1–2 (2019).
- European Commission. *A hydrogen strategy for a climate-neutral Europe*. vol. COM (2020) https://ec.europa.eu/energy/sites/ener/files/hydrogen_strategy.pdf (2020).
- Commonwealth of Australia. *Australia's National Hydrogen Strategy*. (COAG Energy Council Hydrogen Working Group, 2019).
- Bünger, U., Michalski, J., Crotogino, F. & Kruck, O. 7 - Large-scale underground storage of hydrogen for the grid integration of renewable energy and other applications. in *Woodhead Publishing Series in Energy* (eds. Ball, M., Basile, A. & Veziroglu, T. N. B. T.-C. of H. E.) 133–163 (Woodhead Publishing, 2016). <https://doi.org/10.1016/B978-1-78242-364-5.00007-5>.
- Andersson, J. & Grönkvist, S. Large-scale storage of hydrogen. *International Journal of Hydrogen Energy* **44**, 11901–11919 (2019).
- Kruck, O., Crotogino, F., Prelicz, R. & Rudolph, T. Overview on all known underground storage technologies for hydrogen. *Proj. HyUnder-Assessment Potential, Actors Relev. Bus. Cases Large Scale Seas. Storage Renew. Electr. by Hydog. Undergr. Storage Eur. Rep. D* **3**, (2013).
- Zivar, D., Kumar, S. & Foroozesh, J. Underground hydrogen storage: a comprehensive review. *Int. J. Hydrogen Energy* **46**, 23436–23462 (2021).

41. Tarkowski, R., Uliasz-Misiak, B. & Tarkowski, P. Storage of hydrogen, natural gas, and carbon dioxide – Geological and legal conditions. *Int. J. Hydrogen Energy* **46**, 20010–20022 (2021).
42. AEMO. *AEMO costs and technical parameter review Report Final Rev 4 9110715*. (2018).
43. Schmidt, O. et al. Future cost and performance of water electrolysis: An expert elicitation study. *Int. J. Hydrogen Energy* **42**, 30470–30492 (2017).
44. Götz, M. et al. Renewable Power-to-Gas: a technological and economic review. *Renewable Energy* **85**, 1371–1390 (2016).
45. AEMO. *2020 Integrated System Plan For the National Electricity Market*. https://www.aemo.com.au/-/media/Files/Electricity/NEM/Planning_and_Forecasting/ISP/2018/Integrated-System-Plan-2018_final.pdf (2020).
46. Australian Energy Regulator. *State of the Energy Market 2021*. <http://www.aer.gov.au/node/18959> (2021).
47. Government of Western Australia. Initial results confirm Oakajee as ideal site for green hydrogen. *Media Statements* <https://www.mediastatements.wa.gov.au/Pages/McGowan/2021/05/Initial-results-confirm-Oakajee-as-ideal-site-for-green-hydrogen.aspx> (2021).
48. Intercontinental Energy. Asian renewable energy hub. <https://intercontinentalenergy.com/asian-renewable-energy-hub>.
49. ARUP Australia. *Australian Hydrogen Hubs Study: Technical Study*. (2019).
50. Northern Territory Minister for Renewables and Energy. Media Release. *Northern Territory Government Newsroom* <https://newsroom.nt.gov.au/mediaRelease/34187> (2021).
51. Sun Cable Pte Ltd. Australia-ASEAN Power Link. <https://suncable.sg/australia-asean-power-link/>.
52. Feitz, A. J., Tenthorey, E. & Coghlan, R. *Prospective Hydrogen Production Regions of Australia*. *Record* 2019/15. <https://doi.org/10.11636/Record.2019.015%0D> (2019).
53. Ennis-King, J., Michael, K., Strand, J., Regina, S. & Green, C. *Underground storage of Hydrogen: Mapping out the options for Australia*. (2021).
54. Dc/ac ratio and inverter losses. *Renewables.ninja*. <https://community.renewables.ninja/t/dc-ac-ratio-and-inverter-losses/779> (2018).
55. Aurecon & AEMO. *2020 Costs and Technical Parameter Review*. https://www.aemo.com.au/-/media/Files/Electricity/NEM/Planning_and_Forecasting/Inputs-Assumptions-Methodologies/2019/Aurecon-2019-Cost-and-Technical-Parameters-Review-Draft-Report.PDF (2020).
56. AEMO. 2020 Integrated System Plan database. <https://aemo.com.au/energy-systems/major-publications/integrated-system-plan-isp/2020-integrated-system-plan-isp/2019-isp-database>.

Acknowledgements

The work was supported by the Australian Research Council (ARC) Training Centre for The Global Hydrogen Economy (IC200100023).

Author contributions

M.H.A.K., R.D., I.M. and R.A. initially perceived and designed the study. M.H.A.K., P.H. and A.K. collected the data, developed the tools and code, conducted the analysis, and collected the results. M.H.A.K. analysed the data and conducted the theoretical research. M.H.A.K. and A.K. developed the figures. R.D. and I.M. verified the analysis, tools, and theoretical discussion. All authors wrote and reviewed the manuscript.

Competing interests

The authors declare no competing interests.

Additional information

Supplementary information The online version contains supplementary material available at <https://doi.org/10.1038/s43247-022-00640-1>.

Correspondence and requests for materials should be addressed to Rahman Daiyan or Iain MacGill.

Peer review information *Communications Earth & Environment* thanks Rita Alves, Christina Wulf and the other, anonymous, reviewer(s) for their contribution to the peer review of this work. Primary Handling Editors: Omar Asensio, Clare Davis, Heike Langenberg.

Reprints and permission information is available at <http://www.nature.com/reprints>

Publisher's note Springer Nature remains neutral with regard to jurisdictional claims in published maps and institutional affiliations.



Open Access This article is licensed under a Creative Commons Attribution 4.0 International License, which permits use, sharing, adaptation, distribution and reproduction in any medium or format, as long as you give appropriate credit to the original author(s) and the source, provide a link to the Creative Commons license, and indicate if changes were made. The images or other third party material in this article are included in the article's Creative Commons license, unless indicated otherwise in a credit line to the material. If material is not included in the article's Creative Commons license and your intended use is not permitted by statutory regulation or exceeds the permitted use, you will need to obtain permission directly from the copyright holder. To view a copy of this license, visit <http://creativecommons.org/licenses/by/4.0/>.

© The Author(s) 2022